

Exact Standard model structures from Intersecting D5-Branes

Christos Kokorelis

Dep/to de Física Teórica C-XI and Instituto de Física Teórica C-XVI ,
Universidad Autónoma de Madrid, Cantoblanco, 28049, Madrid, Spain

ABSTRACT

We discuss the appearance of non-supersymmetric compactifications with exactly the Standard Model (SM) at low energies, in the context of IIB orientifold constructions with D5 branes intersecting at angles on the T^4 tori, of the orientifold of $T^4 \times (\mathbf{C}/Z_N)$. We discuss constructions where the Standard Model embedding is considering within four, five and six stacks of D5 branes. The appearance of the three generation observable Standard Model at low energies is accompanied by a gauged baryon number, thus ensuring automatic proton stability. Also, a compatibility with a low scale of order TeV is ensured by having a two dimensional space transverse to all branes. The present models complete the discussion of some recently constructed four stack models of D5 branes with the SM at low energy. By embedding the four, five and six stack Standard Model configurations into quiver diagrams, deforming them around the QCD intersection numbers, we find a rich variety of vacua that may have exactly the Standard Model at low energy. Also by using brane recombination on the $U(1)$'s, we show that the five and six vacua flow into their four stack counterparts. Thus string vacua with five and six stack deformations are continuously connected to the four stack vacua.

1 Introduction

One of the main objectives of current string theory research, in the absence of a dynamical mechanism that can select a particular string vacuum, is the search for particular string vacua which can give us at low energies, the observable chiral spectrum of the Standard Model (SM) and gauge interactions. In this sense, semirealistic four dimensional (4D) models have been examined both in $N = 1$ heterotic compactifications and in orientifold constructions [1].

In this work, we will examine standard model compactifications in the context of some recent constructions [2] which use intersecting branes [3, 4] and give 4D non-supersymmetric (non-SUSY) models. At present non-SUSY models are considered a necessity in the search of realistic 4D string models. This is to be contrasted with past research, where the majority of the relevant for phenomenology models considered, were preserving $\mathcal{N} = 1$ supersymmetry in four dimensions. Past model building studies in the context of $N = 1$ weak coupling heterotic orbifold compactifications (HOC), gave rise to semirealistic supersymmetric model generation that included at low energy the MSSM particle content, accompanied by a variety of exotic matter representations and gauge group factors. Additional problems included, among others, the fact that it was not possible to reconcile the observed discrepancy between the unification of gauge couplings in the MSSM at 10^{16} GeV [1] and the string scale at HOC which is of order $10^{17} - 10^{18}$ GeV, even though the latter discrepancy was attributed to the string one loop corrections of the $N = 1$ gauge coupling constants [5]. Thus the failure of obtaining realistic string compactifications in the context of heterotic strings directed research towards orientifold constructions and type IIB constructions with D-branes at singularities. See for example [6, 7, 8, 9, 10, 11, 12, 13]. In general these compactifications are accompanied by extra matter.

However, recent results, that made use of the fact that in type I compactifications (IC) the string scale is a free parameter, suggested that it is possible in IC to lower the string scale, thus solving the hierarchy problem, by having some compact directions transverse to all stacks of branes, in the TeV region even without SUSY [14]. That alone changed the way that we view non-SUSY models, thus suggesting us that non-SUSY models with a string scale in the TeV range is a strong alternative to SUSY models. In this context, the only question remaining is to find realistic compactification examples, giving at low energies exactly the observable SM. As we will see in a moment, the latter was shown that is possible in the context of intersecting branes.

In intersecting brane models the fermions get localized in the intersections between

branes [15]. In these constructions the introduction of a quantized NS-NS B field [16] effectively produces semirealistic models with three generations [4]. These backgrounds are T-dual to models with magnetic deformations [17]. For additional non-SUSY constructions and recent developments in the context of intersecting branes, see [18, 19, 20, 21, 22, 23, 24, 25, 26, 27, 28]. For some new directions in the context of D6 intersecting branes in backgrounds of Calabi-Yau 3-folds see [29]. For backgrounds with intersecting D6-branes on non-compact Calabi-Yau 3-folds see [30]. For a $N = 1$ SUSY construction in the context of intersecting branes and its phenomenology see [31].

Quite recently, a class of models, with four stacks of branes, was presented that gives at low energies exactly the SM content [32]. These models were based on D6-branes intersecting at angles on an orientifolded six-torus compactification [3, 4]. These models have been generalized, to the same D6-brane backgrounds, to classes of models with five- [33] and six-stacks of branes [34] at the string scale that give exactly the SM at low energies. The models of [32, 33, 34] share some interesting common features such as a gauged baryon, with a stable proton, and lepton number symmetries ¹ small neutrino masses and a remarkable Higgs sector that, for some choices of brane angle parameters, is similar of MSSM. However, we should note that, while the non-SUSY four stack model has a variety of sectors where the non-SUSY chiral fields of the SM get localized, models that have five-[33], six-stacks [34] of D6 branes have one additional unusual feature. They have some sectors that preserve $N = 1$ SUSY, even though the model is overall a non-SUSY one. The usefulness of $N = 1$ SUSY sectors stems from the fact that their presence guarantees the presence of singlet scalars, superpartners of right handed neutrinos, ν_R 's, necessary for the breaking of extra $U(1)$ symmetries. In this respect the five, six stack models, uniquely predict the existence of SUSY particles from non-SUSY SM's.

Moreover, the models of [32], [33], [34] have been extended to describe the first examples of string GUT models that give exactly the SM at low energies [35]. The latter classes of models are based on the Pati-Salam [36] gauge group $SU(4) \otimes SU(2)_L \otimes SU(2)_R$ and have a four stack structure at the string scale. They maintain essential features of [32, 33, 34] and in particular the fact that proton is stable, as the baryon number is an unbroken gauged symmetry, and small neutrino masses. Also the GUT four-stack classes of models share the unusual features of the five-, six- stack classes of

¹The corresponding gauge bosons become massive through $B \wedge F$ couplings, arising on a generalized Green-Schwarz mechanism [19, 32, 37, 38]. Thus the associated gauge symmetries survive as global symmetries to low energies.

SM's of [33, 34] respectively, namely they allow SUSY sectors to exist. These models provide us with a nice realization of the see-saw mechanism.

It is quite interesting to note that, even though it was generally believed that in D6 brane orientifolded six torus models it was not possible to find an apparent explanation for lowering the string scale in the TeV region, in the classes of GUT models of [35] this issue was solved differently. In particular, the models predict the existence of light weak doublets with mass of order v^2/M_s , that necessarily needs the string scale to be less than 650 GeV. The latter results are particularly encouraging as they represent strong predictions for D-brane scenarios and are directly testable at present or future accelerators.

In this work, we will discuss compactifications of intersecting D5 branes, that use four-, five- and six-stacks of D5-branes on an orientifolded $T^4 \otimes C/Z_N$ [2]. The classes of models that may potentially give only the SM at low energy are made from four stacks of D5's.

First we discuss again the appearance of exactly the SM at low energy from four stacks of branes. For each of the, four stack, quivers of [2], that give rise to a different class of exactly the SM at low energy ², we present 'alternative' parametric solutions to the twisted RR tadpole cancellation conditions. Moreover, we discuss four new 'reflected' quivers ³ that give rise to the SM at low energy. These 'reflected' quivers are obtained from the ai-type quivers by keeping the Z_N quiver transformation properties of the nodes fixed, while simultaneously interchanging the brane/orientifold content of the nodes with Z_N transformation properties different from unity. Moreover, we show that 'reflected' quivers give SM vacua that are equivalent and in a one to one correspondence to the quivers of [2]. The comparison of the different SM vacua is most easily seen, between the quiver vacua *ai* coming from the alternative RR tadpole solutions and the ones associated with the 'reflected' quivers *Qi*.

We also discuss the embedding of the SM into five and six stacks of D5 Z_3 quivers.

The new classes of SM's exhibit some general features:

- The models are non-SUSY and in the low energies we have apart from the SM spectrum, and gauge interactions, the natural appearance of some scalars fields in various colour and singlet representations. The colour scalars, which have a tachyonic mass in some cases, may obtain a positive mass from one loop effects.

Also present are some singlet scalars that receive a vev and thus break the extra

²denoted as ai-type, ($i = 1, \dots, 4$), and seen in figure (2)

³, denoted as of Qi-type, ($i = 1, \dots, 4$), and seen in figure (1),

anomaly free $U(1)$, beyond hypercharge.

- Baryon number (B) is a gauged $U(1)$ symmetry, thus proton is stable. The corresponding gauge bosons become massive from a dimensional reduction mechanism [2] resembling previously discussed constructions [19].
- The placement of SM chiral fermions to the different intersections inside the four-, five- and six stack D5-brane structure, is exactly the one used in the four-, five and six stack counterpart D6-models of [32, 33, 34] respectively.
- The models may have a low string scale $M_s \sim 1$ TeV, in the way suggested in [14], as there is a transverse compact two dimensional manifold transverse to all D5 branes, whose size may vary, providing for the hierarchy difference between M_{Planck} and M_s .
- The four stack quivers have exactly the observable SM at low energies ⁴. They are classified according to their brane transformation properties under the Z_N orbifold action, schematically seen, by placing the branes and their orientifolded images in various quiver diagrams in the spirit of [39, 40, 41]. As a particular example, in this work we examine in detail the SM embedding in Z_3 quiver diagrams. The five stack and six stack Z_3 quivers ⁵ provide us with more SM-like examples with exactly the SM at low energies. In the latter constructions e.g. A1, C1 C2 additional anomaly free $U(1)$'s orthogonal to hypercharge become massive through the presence of singlet scalars getting a vev.
- Using brane recombination we are able to show that five and six stack string vacua with intersecting D5-branes ‘flow’ to their associated four stack quivers (see sect. 7).

The paper is organized as follows. In the next section we describe the rules, as well the constraints coming from RR tadpole cancellation conditions, for constructing the intersecting at angles D5-brane models in an orientifolded $T^4 \times C/Z_N$ IIB background. In section 3 we describe the exact form of the chiral SM fermionic structure configurations that all the SM's reproduce at low energies. We describe the SM embedding in a four-, five- and six stack D5 structure, which follow from past discussions in [32], [33], [34], respectively.

⁴They also involve the appearance of tachyonic colour singlets that may be expected to receive non-trivial loop corrections.

⁵Any tachyonic scalars present receive loop corrections that list their mass to positive values.

In section 4, we discuss the four stack Z_3 ‘reflected’ quiver embedding of the three generation (3G) SM. We start by discussing the Q1-quiver, presenting in detail the cancellation of the mixed $U(1)$ gauge anomalies by a dimensional reduction scheme which is equivalent to the cancellation of the field theory anomaly by its Green-Schwarz amplitude. This mechanism [2] is an extension of a similar mechanism used in the context of toroidal models with branes at angles in [19]. Also, we discuss the rest of quivers, of Q2, Q3, Q4 type, giving only the SM at low energies. Next we discuss the alternative RR twisted tadpole cancellation conditions to the a-type quivers of [2]. We show that the reflected quivers Qi give equivalent vacua at low energy to their ‘images’ ai -type quivers.

In section 5, we discuss the five stack SM embedding in Z_3 quivers. We discuss a number of quivers characterized as belonging to the A1, $\overline{A1}$, A2, $\overline{A2}$ -quivers. The rest of five stack quivers are examined in Appendix I. For the case of A1-quiver we examine in detail the Higgs sector giving our emphasis on the definition of the geometrical quantities that characterize the geometry of the Higgs sector of the model. Also we discuss the scalar sector of the A1-quiver class of SM’s. Three more examples of five stack quivers are examined in Appendix I.

In section 6, we discuss two examples of six stack SM-like quivers providing more examples with the SM gauge group at low energy in addition to colour and singlet scalars.

In section 7, we make novel use of brane recombination to show the equivalence of six, five and four stack vacua.

Our conclusions together with some comments are presented in section 8. In appendix II, we list the RR tadpole solutions of all the SM embeddings in five stack quivers not examined explicitly in the main body of the paper. In appendix III we list the RR tadpole solutions of all the SM embeddings in six stack quivers, even though only two examples are explicitly examined in the main body of the paper.

2 Exact Standard model structures from Intersecting branes

In this work, we are going to describe new type IIB compactification vacua that have at low energy just the observable Standard Model gauge group and chiral content. The proposed three generation SM’s make use of four, five and six-stacks of D5 branes, intersecting at angles, at the string scale. They are based on the following compactification

[2] scheme

$$IIB/\left(\frac{T^4 \times C/Z_N}{\{1 + \Omega\mathcal{R}\}}\right), \quad (2.1)$$

where Ω is the worldvolume parity and the presence of the parity \mathcal{R} involution is associated to the reflections \mathcal{R}_i of the i -th coordinate, namely $\mathcal{R} = \mathcal{R}_{(5)}\mathcal{R}_{(7)}\mathcal{R}_{(8)}\mathcal{R}_{(9)}$. In a compact form the action of \mathcal{R} on the coordinates could be expressed alternatively by using complex coordinates $Z_i = X_{2i+2} + X_{2i+3}$, $i = 1, 2, 3$. In this case, the presence of \mathcal{R} is more elegantly expressed as

$$\mathcal{R} : Z_i \rightarrow \bar{Z}_i, \quad i = 1, 2; \quad Z_3 \rightarrow \bar{Z}_3. \quad (2.2)$$

The presence of tadpoles induced by the presence of the orientifold planes is cancelled by the introduction of N-stacks of D5 branes ⁶. The latter wrap 2-cycles across the four dimensional tori, while they are located at the tip of the orientifold singularity. We note that under T-duality these constructions are dual to D7-branes with fluxes across the compact T^4 dimensions.

The general picture involves D5_a-branes wrapping 1-cycles (n_a^i, m_a^i) , $i = 1, 2$ along each of the i th- T^2 torus of the factorized T^4 torus, namely $T^4 = T^2 \times T^2$. Thus we allow the four-torus to wrap factorized 2-cycles, so we can unwrap the 2-cycle into products of two 1-cycles, one for each T^2 . The definition of the homology of the 2-cycles as

$$[\Pi_a] = \prod_{i=1}^2 (n_a^i[a_i] + m_a^i[b_i]) \quad (2.3)$$

defines consequently the 2-cycle of the orientifold images as

$$[\Pi_{a^*}] = \prod_{i=1}^2 (n_a^i[a_i] - m_a^i[b_i]). \quad (2.4)$$

We note that because of the $\Omega\mathcal{R}$ symmetry each D5_a-brane 1-cycle, must be accompanied by its $\Omega\mathcal{R}$ orientifold image partner $(n_a^i, -m_a^i)$; $n, m \in Z$. In addition, because of the presence of discrete NS B-flux [16], the tori involved are not orthogonal but tilted. In this way the wrapping numbers become the effective tilted wrapping numbers,

$$(n^i, m = \tilde{m}^i + b^i \cdot n^i/2); \quad n, \tilde{m} \in Z, \quad b^i = 0, 1/2 \quad (2.5)$$

Thus semi-integer values are allowed for the m-wrapping numbers.

Let us now discuss the effect of the orbifold action on the open string sectors. The Z_N orbifold twist in the third complex dimension is generated by the twist vector

⁶Effectively, we will use later $N = 3$.

$v = \frac{1}{N}(0, 0, -2, 0)$, which is fixed by the requirements of modular invariance and for the variety to be spin. The \mathbf{Z}_N action is embedded in the $U(N_a)$ degrees of freedom emanating from the a^{th} stack of D5-branes, through the unitary matrix in the form

$$\gamma_{\omega,a} = \text{diag} \left(\mathbf{1}_{N_a^0}, \alpha \mathbf{1}_{N_a^1}, \dots, \alpha^{N-1} \mathbf{1}_{N_a^{N-1}} \right), \quad (2.6)$$

with $\sum_{i=0}^{N-1} N_a^i = N_a$ and $\alpha \equiv \exp(2\pi i/N)$.

As we have already said, in the presence of $\Omega\mathcal{R}$ orientifold action, we need to include sectors where its brane is accompanied by its orientifold image. Let us denote the $\Omega\mathcal{R}$ image of the brane D5_a-brane by $\Omega\mathcal{R}D5_a$ or alternatively as D5_a*.

Thus for example if the D5_a-brane data are given by

$$(n_a^1, m_a^1) \otimes (n_a^2, m_a^2) \\ \gamma_{\omega,a} = \text{diag} \left(\mathbf{1}_{N_a^0}, \alpha \mathbf{1}_{N_a^1}, \dots, \alpha^{N-1} \mathbf{1}_{N_a^{N-1}} \right), \quad (2.7)$$

then the D5_a* data are given by

$$(n_a^1, -m_a^1) \otimes (n_a^2, -m_a^2) \\ \gamma_{\omega,a^*} = \text{diag} \left(\mathbf{1}_{N_a^0}, \alpha^{N-1} \mathbf{1}_{N_a^1}, \dots, \alpha \mathbf{1}_{N_a^{N-1}} \right), \quad (2.8)$$

The closed string sector, can be computed using orbifold techniques. However, as its spectrum will be non-chiral and non-supersymmetric, it will give rise to four dimensional gravitation and thus will be of no interest to us. As far as the twisted closed string sector is concerned it will rise to some tachyons from the NSNS sectors. Thus from the point of view of the low energy spectrum of the theory the closed string sector is not interesting. We thus focus our attention to the open string sector.

The open string spectrum is computed by taking into account the combined geometric plus the Chan-Paton Z_n action [2]. There are a number of different sectors that should be taken into account when computing the chiral spectrum of the models. They include the sectors $D5_a - D5_b$, $D5_a - D5_{b^*}$ and $D5_a - D5_{a^*}$. E.g. because the $D5_a - D5_b$ sector is not constrained by the $\Omega\mathcal{R}$ projection, its spectrum is computed as in orbifold compactifications. Thus we introduce the twist vector $v_\vartheta = (\vartheta_{ab}^1, \vartheta_{ab}^2, 0, 0)$, where $\pi\vartheta_{ab}^i$ is the angle between the branes on the i^{th} torus. Also the states localized in the ab intersection are characterized by the four-dimensional vectors $r + v_\vartheta$ which enter the mass formula

$$\alpha' M_{ab}^2 = \frac{Y^2}{4\pi\alpha'} + N_{bos}(\vartheta) + \frac{(r + v_\vartheta)^2}{2} - \frac{1}{2} + E_{ab}. \quad (2.9)$$

In (2.9), Y is the transverse distance between the branes a, b ; $N_{bos}(\vartheta)$ is the bosonic oscillator contribution and E_{ab} is the vacuum energy

$$E_{ab} = \sum_{i=1}^3 \frac{1}{2} |\vartheta^i| (1 - |\vartheta^i|) . \quad (2.10)$$

The complete massless and tachyonic states reads:

Sector	State	Z_N phase	$\alpha' \text{Mass}^2$	
NS	$(-1 + \vartheta^1, \vartheta^2, 0, 0)$	1	$-\frac{1}{2}(\vartheta^1 - \vartheta^2)$	(2.11)
	$(\vartheta^1, -1 + \vartheta^2, 0, 0)$	1	$\frac{1}{2}(\vartheta^1 - \vartheta^2)$	
R	$(-\frac{1}{2} + \vartheta^1, -\frac{1}{2} + \vartheta^2, -\frac{1}{2}, +\frac{1}{2})$	$e^{2\pi i \frac{1}{N}}$	0	
	$(-\frac{1}{2} + \vartheta^1, -\frac{1}{2} + \vartheta^2, +\frac{1}{2}, -\frac{1}{2})$	$e^{-2\pi i \frac{1}{N}}$	0	

where $\vartheta^i \equiv \vartheta_{ab}^i$ and we have set $0 < \vartheta^i < 1$, $i = 1, 2$. As is it clear from above, one of the NS states will be necessarily tachyonic while the other will have a positive mass. Also, when $|\vartheta^1| = |\vartheta^2|$ the associated state becomes massless. The final spectrum will be found again by projecting to the invariant subspace. We note that the number of chiral fermions localized in the intersection between the a -, b -branes, is given by the intersection number

$$I_{ab} \equiv [\Pi_a] \cdot [\Pi_b] = (n_a^1 m_b^1 - m_a^1 n_b^2)(n_a^2 m_b^2 - m_a^2 n_b^2). \quad (2.12)$$

where its sign denotes the chirality of the corresponding fermion. The full spectrum appearing in the ab -sector is given by

Tachyons	$\sum_{a < b} \sum_{i=1}^N I_{ab} \times (N_a^i, \overline{N}_b^i)$	
Left Fermions	$\sum_{a < b} \sum_{i=1}^N I_{ab} \times (N_a^i, \overline{N}_b^{i+1})$	(2.13)
Right Fermions	$\sum_{a < b} \sum_{i=1}^N I_{ab} \times (N_a^i, \overline{N}_b^{i-1})$	

The complete spectrum for the D5 branes intersecting at angles in the backgrounds (2.1) reads:

Complex Scalars

$$\begin{aligned} & \sum_{a < b} \sum_{i=1}^N [|I_{ab}| (N_a^i, \overline{N}_b^i) + |I_{ab}^*| (N_a^i, N_b^{-i})] \\ & \sum_a [2|m_a^1 m_a^2| (|n_a^1 n_a^2| + 1)(\mathbf{A}_a^0) + 2|m_a^1 m_a^2| (|n_a^1 n_a^2| - 1)(\mathbf{S}_a^0)] \end{aligned}$$

Left Fermions

$$\begin{aligned} & \sum_{a < b} \sum_{i=1}^N [I_{ab} (N_a^i, \overline{N}_b^{i+1}) + I_{ab}^* (N_a^i, N_b^{-i-1})] \\ & \sum_a \sum_{j,i=1}^N \delta_{j,-i-1} [2m_a^1 m_a^2 (n_a^1 n_a^2 + 1)(\mathbf{A}_a^j) + 2m_a^1 m_a^2 (n_a^1 n_a^2 - 1)(\mathbf{S}_a^j)] \end{aligned} \quad (2.14)$$

Right Fermions

$$\begin{aligned} & \sum_{a < b} \sum_{i=1}^N [I_{ab} (N_a^i, \overline{N}_b^{i-1}) + I_{ab}^* (N_a^i, N_b^{-i+1})] \\ & \sum_a \sum_{j,i=1}^N \delta_{j,-i+1} [2m_a^1 m_a^2 (n_a^1 n_a^2 + 1)(\mathbf{A}_a^j) + 2m_a^1 m_a^2 (n_a^1 n_a^2 - 1)(\mathbf{S}_a^j)] \end{aligned}$$

Any vacuum derived from the previous intersection constraints is subject additionally to constraints coming from RR tadpole cancellation conditions. The latter are equivalent to the Gauss law and imply the vanishing of the total RR charge in the compact T^4 space. That demands cancellation of D5-branes charges ⁷, wrapping on two cycles with homology $[\Pi_a]$ and O5-plane 6-form charges wrapping on 2-cycles with homology $[\Pi_{O_5}]$. Note that the RR tadpole cancellation conditions in terms of cancellations of RR charges in homology are expressed as

$$c_k^2 \sum_a ([\Pi_a] \text{Tr} \gamma_{k,a} + [\Pi_{a^*}] \text{Tr} \gamma_{k,a^*}) = [\Pi_{O_5}] 16 \beta^1 \beta^2 \sin \left(\frac{\pi k}{N} \right), \quad (2.15)$$

where $[\Pi_{O_5}]$ describes the 2-cycle of \mathbf{T}^4 the O5-plane wraps, $\beta^i = 1 - b^{(i)}$ parametrizes the NS B-field background and c_k where $c_k^2 = \sin \frac{2\pi k}{N}$ is a weight for each k^{th} twisted sector usually arising in \mathbf{Z}_N orientifold compactifications [42]. Also, $16\beta^1\beta^2$ can be seen as the number of O5-planes, e.g. $4\beta^1\beta^2$, times their relative charge to the D5-brane, e.g. -4 .

In explicit form the tadpoles are given by [2]

$$\begin{aligned} c_k^2 \sum_a n_a^1 n_a^2 (\text{Tr} \gamma_{k,a} + \text{Tr} \gamma_{k,a^*}) &= 16 \sin \left(\frac{\pi k}{N} \right) \\ c_k^2 \sum_a m_a^1 m_a^2 (\text{Tr} \gamma_{k,a} + \text{Tr} \gamma_{k,a^*}) &= 0 \\ c_k^2 \sum_a n_a^1 m_a^2 (\text{Tr} \gamma_{k,a} - \text{Tr} \gamma_{k,a^*}) &= 0 \\ c_k^2 \sum_a m_a^1 n_a^2 (\text{Tr} \gamma_{k,a} - \text{Tr} \gamma_{k,a^*}) &= 0 \end{aligned} \quad (2.16)$$

The presence of a non-zero term in the first tadpole condition should be interpreted as a negative RR charge induced by the presence of an O5-plane. We should note that, alternatively, the first of twisted tadpole conditions can be rewritten as

$$\sum_a n_a^1 n_a^2 (\text{Tr} \gamma_{2k,a} + \text{Tr} \gamma_{2k,a^*}) = \frac{16}{\alpha^k + \alpha^{-k}}. \quad (2.17)$$

3 The D5 Standard Model Configuration's

In this section we will describe the embedding of the SM chiral spectrum into configurations of four-, five, and six- D5-brane stacks. The SM embedding appear in the effective string theories produced by the Z_3 , quiver diagrams giving us a variety of vacua that have the SM at low energy. Our search is facilitated using the four, five of

⁷Taken together with their orientifold images $(n_a^i, -m_a^i)$ wrapping on two cycles of homology class $[\Pi_{\alpha^*}]$.

six stack embedding of the SM chiral fermions that have appeared before in the context of orientifolded intersecting D6 branes [32, 33, 34] respectively. Also we describe the basic characteristics of the classes of SM vacua produced, following their derivation from the various quivers.

3.1 The Standard Model configurations

In this section, we describe the general characteristics of the different SM configurations that we will make use in this work. We will describe models based on a four stack

$$U(3) \otimes U(2) \otimes U(1)_c \otimes U(1)_d , \quad (3.1)$$

a five stack

$$U(3) \otimes U(2) \otimes U(1)_c \otimes U(1)_d \otimes U(1)_e , \quad (3.2)$$

and a six-stack structure

$$U(3) \otimes U(2) \otimes U(1)_c \otimes U(1)_d \otimes U(1)_e \otimes U(1)_f \quad (3.3)$$

at the string scale. The localization of fermions into particular intersections, as seen in table (1), have been considered before in [2] for the four stack D5-models. The complete accommodation of the fermion structure of the chiral SM fermion content in the five- and six-stack SM models in the different open string sectors can be seen in tables (2) and (3).

Several comments are in order:

Matter Fields		Intersection	Q_a	Q_b	Q_c	Q_d	Y
Q_L	$(3, 2)$	I_{ab}	1	-1	0	0	1/6
q_L	$2(3, 2)$	I_{ab^*}	1	1	0	0	1/6
U_R	$3(\bar{3}, 1)$	I_{ac}	-1	0	1	0	-2/3
D_R	$3(\bar{3}, 1)$	I_{ac^*}	-1	0	-1	0	1/3
L	$3(1, 2)$	I_{bd}	0	-1	0	1	-1/2
N_R	$3(1, 1)$	I_{cd}	0	0	1	-1	-1/2
E_R	$3(1, 1)$	I_{cd^*}	0	0	-1	-1	0

Table 1: Low energy fermionic spectrum of the four stack string scale $SU(3)_C \otimes SU(2)_L \otimes U(1)_a \otimes U(1)_b \otimes U(1)_c \otimes U(1)_d$, D5-brane model together with its $U(1)$ charges.

a) We note that there are a number of constraints that the chiral spectra take into account. First of all, as a result of tadpole cancellation conditions, there is an equal

Matter Fields		Intersection	Q_a	Q_b	Q_c	Q_d	Q_e	Y
Q_L	$(3, 2)$	I_{ab}	1	-1	0	0	0	1/6
q_L	$2(3, 2)$	I_{ab^*}	1	1	0	0	0	1/6
U_R	$3(\bar{3}, 1)$	I_{ac}	-1	0	1	0	0	-2/3
D_R	$3(\bar{3}, 1)$	I_{ac^*}	-1	0	-1	0	0	1/3
L	$2(1, 2)$	I_{bd}	0	-1	0	1	0	-1/2
l_L	$(1, 2)$	I_{be}	0	-1	0	0	1	-1/2
N_R	$2(1, 1)$	I_{cd}	0	0	1	-1	0	0
E_R	$2(1, 1)$	I_{cd^*}	0	0	-1	-1	0	1
ν_R	$(1, 1)$	I_{ce}	0	0	1	0	-1	0
e_R	$(1, 1)$	I_{ce^*}	0	0	-1	0	-1	1

Table 2: Low energy fermionic spectrum of the five stack string scale $SU(3)_C \otimes SU(2)_L \otimes U(1)_a \otimes U(1)_b \otimes U(1)_c \otimes U(1)_d \otimes U(1)_e$, D5-brane model together with its $U(1)$ charges.

number of fundamental and anti-fundamental representations. The models necessarily include right handed neutrinos ν_R in the SM spectrum. Thus from now on, when we speak about obtaining the SM at low energies, we will mean the SM with three generations of ν_R 's.

b) The models accommodate various known low energy gauged symmetries. The latter can be expressed in terms of the $U(1)$ symmetries. For example the baryon number, B , is expressed as $B = 3Q_a$ in the four, five and six stacks of models. The study of Green-Schwarz mechanism will show us that baryon number is an unbroken gauged symmetry and as a result the corresponding gauge boson gets massive leaving at low energies the baryon number as a global symmetry. Thus proton is stable.

b) The mixed anomalies A_{ij} of the $U(1)$'s with the non-abelian gauge groups $SU(N_a)$ of the theory cancel through a generalized GS mechanism [19, 37, 38], involving close string modes couplings to worldsheet gauge fields [2]. Two combinations of the $U(1)$'s are anomalous- model independent and become massive, their orthogonal non-anomalous combination survives, combining to a single $U(1)$ that remains massless, the latter to be identified with the hypercharge generator.

c) The hypercharge operator in the model is defined as a linear combination of the $U(1)_a, U(1)_c, U(1)_d, U(1)_e, U(1)_f$ gauge groups for the four-, five-, six-stack models

Matter Fields		Intersection	Q_a	Q_b	Q_c	Q_d	Q_e	Q_f	Y
Q_L	$(3, 2)$	I_{ab}	1	-1	0	0	0	0	1/6
q_L	$2(3, 2)$	I_{ab^*}	1	1	0	0	0	0	1/6
U_R	$3(\bar{3}, 1)$	I_{ac}	-1	0	1	0	0	0	-2/3
D_R	$3(\bar{3}, 1)$	I_{ac^*}	-1	0	-1	0	0	0	1/3
L^1	$(1, 2)$	I_{bd}	0	-1	0	1	0	0	-1/2
L^2	$(1, 2)$	I_{be}	0	-1	0	0	1	0	-1/2
L^3	$(1, 2)$	I_{bf}	0	-1	0	0	0	1	-1/2
N_R^1	$(1, 1)$	I_{cd}	0	0	1	-1	0	0	0
E_R^1	$(1, 1)$	I_{cd^*}	0	0	-1	-1	0	0	1
N_R^2	$(1, 1)$	I_{ce}	0	0	1	0	-1	0	0
E_R^2	$(1, 1)$	I_{ce^*}	0	0	-1	0	-1	0	1
N_R^3	$(1, 1)$	I_{cf}	0	0	1	0	0	-1	0
E_R^3	$(1, 1)$	I_{cf^*}	0	0	-1	0	0	-1	1

Table 3: Low energy fermionic spectrum of the six stack string scale $SU(3)_C \otimes SU(2)_L \otimes U(1)_a \otimes U(1)_b \otimes U(1)_c \otimes U(1)_d \otimes U(1)_e \otimes U(1)_f$, D5-brane model together with its $U(1)$ charges.

respectively:

$$Y = \frac{1}{6}U(1)_a - \frac{1}{2}U(1)_c - \frac{1}{2}U(1)_d . \quad (3.4)$$

$$Y = \frac{1}{6}U(1)_a - \frac{1}{2}U(1)_c - \frac{1}{2}U(1)_d - \frac{1}{2}U(1)_e . \quad (3.5)$$

$$Y = \frac{1}{6}U(1)_a - \frac{1}{2}U(1)_c - \frac{1}{2}U(1)_d - \frac{1}{2}U(1)_e - \frac{1}{2}U(1)_f . \quad (3.6)$$

d) Scalars, massless or tachyonic, appear naturally in the present classes of models. This is to be contrasted with the D6 branes wrapping on T^6 orientifolded constructions [3, 4], where one has to make some open string sectors supersymmetric in order to guarantee the presence of massless scalars in the models. The latter case was most obvious in the construction of $N = 0$ models, with just the SM at low energy from five -[33], six stacks [34] of D6-branes, as well from constructions with a Pati-Salam G_{422} D6 four stack GUT, on the orientifolded T^6 backgrounds [35] at the string scale. The presence of scalars is necessary in order to break the additional massless, beyond the hypercharge, anomaly free $U(1)$'s that survive the Green-Schwarz mechanism.

e) A variety of SM solutions will be presented that are directly related to the embedding of the SM configurations in tables (1), (2), (3) in quiver diagrams. In general, when D-branes are localized on an orbifold singularity \mathbf{C}^n , the description of the local physics at the singularity is obtained by keeping states that are invariant under the the combined geometric and gauge action on the Chan-Paton index by the action of the discrete group Γ acting on the singularity [39, 40, 41].

Each quiver records the action of the orbifold group on the branes and their orientifold images. We chosen for simplicity the orbifold group to be abelian, e.g. a Z_3 , however more general Z_N choices are possible.

We should note that what is important for having the SM at low energy constructions is not the particular Z_N quiver we examine, but rather the four, five, six- stack configuration that localizes the chiral three generation SM fermion content, as seen in tables (1), (2), (3). The structures of tables (1), (2), (3) have been used before in the D6 orientifolded models of [32, 33, 34] respectively.

In a quiver, each arrow between two nodes represents a chiral fermion transforming in the bifundamental representation of the two linked nodes. Also the direction of the arrows denotes the chirality of the representation and we choose left handed fermions to correspond to arrows directed clockwise.

At a four stack level, we found four different Z_3 quiver diagrams, that give rise to exactly the SM at low energies. They are denoted as belonging to the Q1-, Q2- Q3-, Q4-type and they are examined in the next section. Also we provide alternative RR tadpole cancellation conditions, to the ones appearing in [2], for the four stack quivers of a1-, a2-, a3-, a4-type. Also, a number of five stack quivers are being examined that are characterized as belonging to the A1, A2, $\overline{A1}$, $\overline{A2}$ and in Appendix B the B1, B2, B3 type quivers. Moreover the six-stack quivers that are examined are characterized as belonging to the C1, C2 type.

Care should be taken when treating the intersection numbers of a SM embedding. The sign of the intersection number that denotes the chirality of the relevant fermion, depends on the direction of the arrows between the nodes. For example, the following intersection numbers hold in the four stack *a4*-quiver, the five stack *A1*-quiver or the six stack *C2*-quiver respectively :

$$\begin{aligned} I_{ab} &= -1, I_{ab^*} = +2, I_{ac} = -3, I_{cd^*} = +3 \\ I_{bd} &= -3, I_{cd^*} = +3, I_{cd} = -3. \end{aligned} \tag{3.7}$$

$$I_{ab} = +1, I_{ab^*} = -2, I_{ac} = -3,$$

$$\begin{aligned}
I_{ac^*} &= +3, I_{bd} = +2, I_{cd} = -2, I_{cd^*} = +2, \\
I_{be} &= +1, I_{ce} = -1, I_{ce^*} = +1
\end{aligned} \tag{3.8}$$

$$\begin{aligned}
I_{ab} &= +1, I_{ab^*} = -2, I_{ac} = +3, I_{ac^*} = -3, \\
I_{bd} &= +1, I_{be} = +1, I_{bf} = +1, \\
I_{cd} &= +1, I_{cd^*} = -1, I_{ce} = +1, \\
I_{ce^*} &= -1, I_{cf} = 1, I_{cf^*} = -1.
\end{aligned} \tag{3.9}$$

4 Exact SM vacua from Four-Stack Quivers

In this section, we discuss the appearance of exactly the SM at low energy from four stacks of D5 branes. The orbifold structure of the SM configurations will be depicted in terms of quiver diagrams. In particular we examine Z_3 quivers.

Initially, we describe ⁸ the ‘reflected’ quivers seen in figure (1). These four stack quivers give rise to four different classes of SM vacua at low energy. For each of them we show that they give equivalent SM vacua to its ‘image’ ai-quivers seen in figure (2). For the ‘image’ ai-quivers, we discuss alternative RR tadpole solutions, to the one’s that have appeared in [2].

4.1 Exact SM vacua from the ‘reflected’ Q1-Quiver

In this subsection we examine the derivation of exactly the SM at low energies from the embedding of the four stack SM structure of table (1) in a Z_3 quiver of Q1-type.

The solutions satisfying simultaneously the intersection constraints and the cancellation of the RR twisted crosscap tadpole cancellation constraints are given in parametric form in table (4). The multiparameter RR tadpole solutions appearing in table (4) represent deformations of the D5-brane branes, of table (1), intersecting at angles, within the same homology class of the factorizable two-cycles. The solutions of table (4) satisfy all tadpole equations, in (2.16), but the first. The latter reads :

$$9n_a^1 - \frac{1}{\beta^1} + \tilde{\epsilon} n_d^1 + \frac{2\epsilon_h N_h}{\beta^1} = -8. \tag{4.1}$$

Note that we had added the presence of extra N_h branes. Their contribution to the RR tadpole conditions is best described by placing them in the three-factorizable cycle

$$N_h (\epsilon_h/\beta_1, 0) (2, 0) 1_{N_h}. \tag{4.2}$$

⁸, what was described in the introduction as,

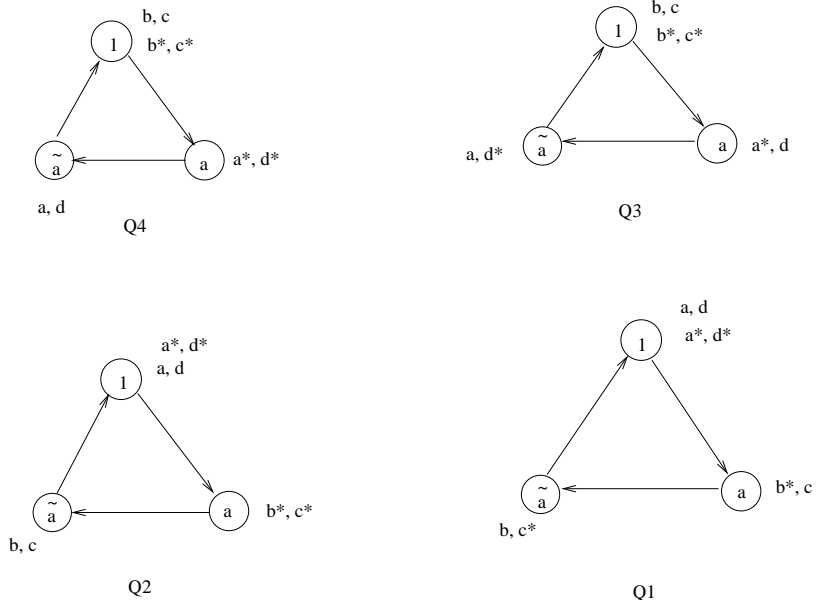


Figure 1: Assignment of SM embedding in configurations of four stacks of D5 branes depicted by the ‘reflected’ Z_3 quiver diagrams. At low energy we get only the SM. Note that $\tilde{\alpha} = \alpha^{-1}$. These configurations give equivalent vacua, with exactly the SM at low energy, to those vacua coming from the ‘image’ quivers of figure (2), under the correspondence $a1 \iff Q1$, $a2 \iff Q2$, $a3 \iff Q3$, $a4 \iff Q4$.

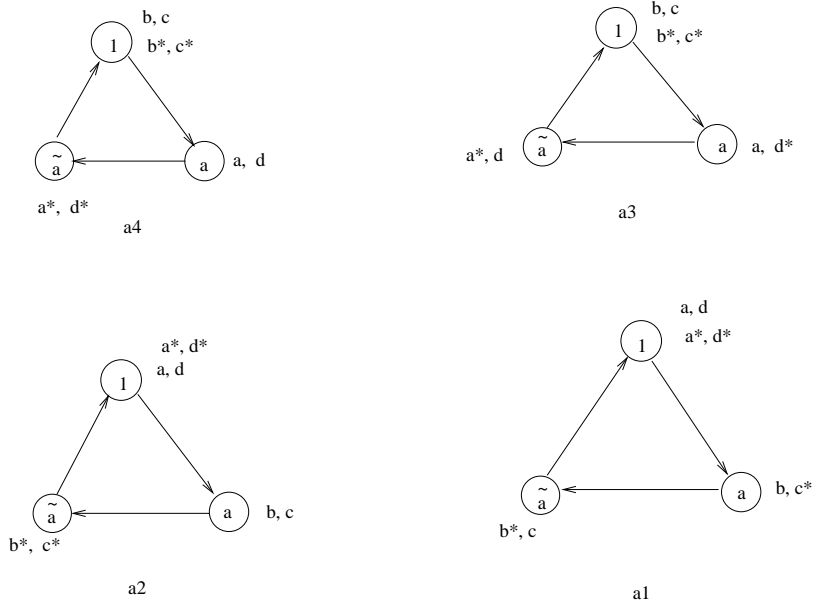


Figure 2: Assignment of SM embedding in configurations of four stacks of D5 branes depicted by Z_3 quiver diagrams. At low energy we get only the SM. Note that $\tilde{\alpha} = \alpha^{-1}$.

N_i	(n_i^1, m_i^1)	(n_i^2, m_i^2)	(n_i^3, m_i^3)
$N_a = 3$	$(n_a^1, \epsilon \tilde{\epsilon} \beta^1)$	$(3, \frac{1}{2} \tilde{\epsilon} \epsilon)$	1_3
$N_b = 2$	$(1/\beta_1, 0)$	$(1, \frac{1}{2} \epsilon \tilde{\epsilon})$	$\alpha^2 \mathbf{1}_2$
$N_c = 1$	$(1/\beta_1, 0)$	$(0, \epsilon \tilde{\epsilon})$	α
$N_d = 1$	$(n_d^1, 3\epsilon \beta^1)$	$(\tilde{\epsilon}, -\frac{1}{2} \epsilon)$	1
N_h	$(\epsilon_h/\beta^1, 0)$	$(2, 0)$	1_{N_h}

Table 4: General tadpole solutions for the four-stack $Q1$ -type quiver of intersecting D5-branes, giving rise to exactly the standard model gauge group and observable chiral spectrum at low energies. The solutions depend on two integer parameters, n_a^1, n_d^1 , the NS-background $\beta^1 = 1 - b_i$, which is associated to the presence of the NS B-field by $b_i = 0, 1/2$. and the phase parameters $\epsilon = \tilde{\epsilon} = \pm 1$, as well as the CP phase α .

The presence of an arbitrary number of N_h D5-branes, which give an extra $U(N_h)$ gauge group, don't make any contribute to the rest of the tadpoles and intersection constraints. Thus in terms of the low energy theory their presence has no effect and only the SM appears.

Most of the gauge theory anomalies of the four $U(1)$'s of the models cancel as a consequence of the tadpole cancellation conditions. As was shown in [2], the cubic non-abelian anomaly cancels as a consequence of the tadpole cancellation conditions. The mixed $U(1) - SU(N)^2$ anomaly partially cancels, as a consequence of the tadpole cancellation conditions while a non-cancelled piece remains, namely

$$\mathcal{A}_{U(1)_{a,i} - SU(N_b^j)^2} = \frac{-2N_a^i}{N} \sum_{k=1}^N e^{2\pi i \frac{k \cdot i}{N}} c_k^2 \left(I_{ab} e^{-2\pi i \frac{k \cdot j}{N}} + I_{ab^*} e^{2\pi i \frac{k \cdot j}{N}} \right). \quad (4.3)$$

The latter cancels [19] by the exchange of four-dimensional fields, which come from the dimensional reduction of the RR twisted forms living on the singularity [2]. This is clearly seen in the T-dual picture of fractional D7-branes wrapping the first two tori in the presence of non-trivial F and B -fluxes. By integrating the couplings of the twisted RR p-forms ⁹ of even p, A_0, A_2, A_4, A_6 , over the compact dimensions $(\mathbf{T}^2)_1 \times (\mathbf{T}^2)_2$,

⁹Appearing in the worldvolume of each D7-brane.

we can defining the fields [2]

$$\begin{aligned}
B_0^{(k)} &= A_0^{(k)}, & B_2^{(k)} &= \int_{(\mathbf{T}^2)_1 \times (\mathbf{T}^2)_2} A_6^{(k)}, \\
C_0^{(k)} &= \int_{(\mathbf{T}^2)_1 \times (\mathbf{T}^2)_2} A_4^{(k)}, & C_2^{(k)} &= A_2^{(k)}, \\
D_0^{(k)} &= \int_{(\mathbf{T}^2)_2} A_2^{(k)}, & D_2^{(k)} &= \int_{(\mathbf{T}^2)_1} A_4^{(k)}, \\
E_0^{(k)} &= \int_{(\mathbf{T}^2)_1} A_2^{(k)}, & E_2^{(k)} &= \int_{(\mathbf{T}^2)_2} A_4^{(k)}.
\end{aligned} \tag{4.4}$$

derive the four dimensional couplings as

$$\begin{aligned}
& c_k N_a^i n_a^1 n_a^2 \int_{M_4} \text{Tr} (\gamma_{k,a} - \gamma_{k,a^*}) \lambda_i B_2^{(k)} \wedge \text{Tr} F_{a,i}, \\
& c_k N_a^i m_a^1 m_a^2 \int_{M_4} \text{Tr} (\gamma_{k,a} - \gamma_{k,a^*}) \lambda_i C_2^{(k)} \wedge \text{Tr} F_{a,i}, \\
& c_k N_a^i n_a^1 m_a^2 \int_{M_4} \text{Tr} (\gamma_{k,a} + \gamma_{k,a^*}) \lambda_i D_2^{(k)} \wedge \text{Tr} F_{a,i}, \\
& c_k N_a^i m_a^1 n_a^2 \int_{M_4} \text{Tr} (\gamma_{k,a} + \gamma_{k,a^*}) \lambda_i E_2^{(k)} \wedge \text{Tr} F_{a,i},
\end{aligned} \tag{4.5}$$

$$\begin{aligned}
& c_k m_a^1 m_a^2 \int_{M_4} \text{Tr} (\gamma_{k,a}^{-1} + \gamma_{k,a^*}^{-1}) \lambda_j^2 B_0^{(k)} \wedge \text{Tr} (F_{a,j} \wedge F_{a,j}), \\
& c_k n_a^1 n_a^2 \int_{M_4} \text{Tr} (\gamma_{k,a}^{-1} + \gamma_{k,a^*}^{-1}) \lambda_j^2 C_0^{(k)} \wedge \text{Tr} (F_{a,j} \wedge F_{a,j}), \\
& c_k m_a^1 n_a^2 \int_{M_4} \text{Tr} (\gamma_{k,a}^{-1} - \gamma_{k,a^*}^{-1}) \lambda_j^2 D_0^{(k)} \wedge \text{Tr} (F_{a,j} \wedge F_{a,j}), \\
& c_k n_a^1 m_a^2 \int_{M_4} \text{Tr} (\gamma_{k,a}^{-1} - \gamma_{k,a^*}^{-1}) \lambda_j^2 E_0^{(k)} \wedge \text{Tr} (F_{a,j} \wedge F_{a,j}),
\end{aligned} \tag{4.6}$$

where λ is the Chan-Paton wavefunction for the gauge boson state, and N_a^i factor arises from normalization of the $U(1)_{a,i}$ generator. Since $B_2^{(k)}$, $C_2^{(k)}$, $D_2^{(k)}$ and $B_0^{(k)}$, $C_0^{(k)}$, $D_0^{(k)}$ are four-dimensional Hodge duals respectively, the sum over the GS diagrams contributes a counterterm that provides us with the structure required to cancel the residual mixed anomaly (4.3).

In order to compute the twisted RR couplings for a specific model, that means taking into account the $U(1)$ anomaly constraints of (4.5, 4.6), we should take into consideration the number of twisted sectors available to us. For the Z_3 orientifold quivers that we examine in this work there is only one independent twisted sector. Thus for the Q1-quiver the constraints from $U(1)$ anomaly cancellation appear into three terms

$$\begin{aligned}
& B_2^{(1)} \wedge c_1 \left(\frac{2(\alpha^2 - \alpha)}{\beta^1} \right) F^b, \\
& D_2^{(1)} \wedge c_1 [\epsilon \tilde{\epsilon}] \left(3n_a^1 F^a - \frac{1}{\beta^1} F^b - \frac{1}{\beta^1} F^c - \tilde{\epsilon} n_d^1 F^d \right), \\
& E_2^{(1)} \wedge c_1 [6\epsilon \tilde{\epsilon} \beta^1] [3F^a + F^d].
\end{aligned} \tag{4.7}$$

From (4.7) we conclude that there are two non-anomalous $U(1)$'s that become massive through their couplings to the RR fields. They are the model independent fields, $U(1)_b$ and the combination $3U(1)_a + U(1)_d$, which become massive through their

couplings to the RR 2-form fields $B_2^{(1)}, E_2^{(1)}$ respectively. In addition, there is a model dependent anomalous and massive $U(1)$ field coupled to $D_2^{(1)}$ field. That means that the two non-anomalous free combinations are $U(1)_c$ and $U(1)_a - 3U(1)_d$.

Thus the combination of the $U(1)$'s, having no couplings to twisted RR fields, remains light to low energies is

$$Q^l = (Q_a - 3Q_d) + 3\beta^1(n_a^1 + \tilde{\epsilon}n_d^1)Q_c. \quad (4.8)$$

The subclass of tadpole solutions of (4.8) having the SM hypercharge assignment at low energies is exactly the one which is proportional to (3.4). It satisfies the condition,

$$\beta_1 (n_a^1 + \tilde{\epsilon}n_d^1) = -1. \quad (4.9)$$

Summarizing, as long as (4.9) holds the $U(1)$ (4.8) is the hypercharge generator of the SM. Thus at low energies we get the chiral fermion content of the SM that gets localized according to the open string sectors appearing in table (1).

An alternative RR tadpole solution for the Q1-quiver class of SM's can be seen in table (5).

N_i	(n_i^1, m_i^1)	(n_i^2, m_i^2)	(n_i^3, m_i^3)
$N_a = 3$	$(n_a^1, -\epsilon\tilde{\epsilon}\beta^1)$	$(3, -\frac{1}{2}\tilde{\epsilon}\epsilon)$	1_3
$N_b = 2$	$(1/\beta_1, 0)$	$(1, -\frac{1}{2}\epsilon\tilde{\epsilon})$	$\alpha^2 \mathbf{1}_2$
$N_c = 1$	$(1/\beta_1, 0)$	$(0, -\epsilon\tilde{\epsilon})$	α
$N_d = 1$	$(n_d^1, 3\epsilon\beta^1)$	$(-\tilde{\epsilon}, -\frac{1}{2}\epsilon)$	1
N_h	$(\epsilon_h/\beta^1, 0)$	$(2, 0)$	1_{N_h}

Table 5: Alternative general tadpole solutions for the four-stack Q1-type quiver of intersecting D5-branes, giving rise to exactly the standard model gauge group and observable chiral spectrum at low energies. The solutions depend on two integer parameters, n_a^1, n_d^1 , the NS-background β^1 and the phase parameters $\epsilon = \tilde{\epsilon} = \pm 1$, as well as the CP phase α .

In this case the $U(1)$ couplings to twisted RR fields read

$$B_2^{(1)} \wedge c_1[2\frac{(\alpha^2 - \alpha)}{\beta^1}]F^b,$$

$$\begin{aligned}
D_2^{(1)} \wedge c_1[\epsilon\tilde{\epsilon}][&-3n_a^1 F^a + \frac{1}{\beta^1} F^b + \frac{1}{\beta^1} F^c - \tilde{\epsilon} n_d^1 F^d], \\
E_2^{(1)} \wedge c_1[&-6\epsilon\tilde{\epsilon}\beta^1][3F^a + F^d].
\end{aligned} \tag{4.10}$$

With the choice of tadpole solutions of table (5) all tadpole equations in (2.16) are satisfied but the first, the latter giving

$$9n_a^1 - \frac{1}{\beta^1} - \tilde{\epsilon} + \frac{2\epsilon_h N_h}{\beta^1} = -8. \tag{4.11}$$

The combination of the $U(1)$'s

$$Q^l = (Q_a - 3Q_d) + 3\beta^1(n_a^1 - \tilde{\epsilon}n_d^1)Q_c. \tag{4.12}$$

if the hypercharge condition

$$\beta^1(n_a^1 - \tilde{\epsilon}n_d^1) = -1. \tag{4.13}$$

is fulfilled is the hypercharge.

4.2 Scalar sector of the ‘reflected’ Q1-quiver

In this class of models, the scalars appear from the aa^* , ad^* , ad sectors. Lets us make a particular choice of the tadpole parameters on these SM's taking into account the constraints (4.1), (4.9). We choose

$$n_a^1 = -1, \quad n_d^1 = -1, \quad \beta^1 = 1/2, \quad \epsilon_h = 1, \quad N_h = 2, \quad \epsilon = 1, \quad \tilde{\epsilon} = 1 \tag{4.14}$$

Sector	Representation	$\alpha' \cdot mass^2$
aa^*	$2(3, 1)_{1/3} + (6, 1)_{-1/3}$	$\pm \frac{1}{\pi} \left(\tan^{-1} \left(\frac{U^1}{2} \right) - \tan^{-1} \left(\frac{U^2}{6} \right) \right) \xrightarrow{U^1 = \frac{U^2}{3}} 0$
ad	$4(3, 1)_{2/3}$	$\pm \frac{1}{2\pi} \left[\tan^{-1} \left(\frac{3U^1}{2} \right) - \tan^{-1} \left(\frac{U^1}{2} \right) - \tan^{-1} \left(\frac{U^2}{6} \right) - \right. \\ \left. \tan^{-1} \left(\frac{U^2}{2} \right) \right] \xrightarrow{U^1 = \frac{U^2}{3}} \pm \frac{1}{\pi} \tan^{-1} \left(\frac{U^2}{6} \right)$
ad^*	$2(3, 1)_{-1/3}$	$\pm \frac{1}{2\pi} \left[-\frac{1}{\pi} \tan^{-1} \left(\frac{U^1}{2} \right) - \tan^{-1} \left(\frac{3U^1}{2} \right) + \tan^{-1} \left(\frac{U^2}{2} \right) - \right. \\ \left. \tan^{-1} \left(\frac{U^2}{6} \right) \right] \xrightarrow{U^1 = \frac{U^2}{3}} \pm \frac{1}{\pi} \tan^{-1} \left(\frac{U^2}{6} \right)$

Table 6: Lightest scalar excitations for the four stack Q1-quiver SM's.

There are two issues that might concern us at this point. The first one has to do with the existence of tachyons. By choosing $U^1 = U^2/3$ the mass of the colour

aa^* -sector goes to zero while the scalars from the ad , ad^* -sectors can get tachyonic values. However, as has been emphasized in [2], the last problem may be avoided as scalars may receive loop corrections from one gauge boson exchange in the form that may stronger for colour scalars. These corrections could drive their masses to positive values (See also subsection (5.3)). The lighter scalar excitations for this class of SM's can be seen in table (6).

4.3 Exact SM vacua from the ‘reflected’ Q2-Quiver

This is another class of models which may have exactly the SM at low energy as the scalars appearing are coloured and thus we expect loop corrections to lift the tachyonic directions. In this subsection we examine the derivation of exactly the SM at low energies from the embedding of the four stack SM structure of table (1) in a Z_3 quiver of Q2-type.

N_i	(n_i^1, m_i^1)	(n_i^2, m_i^2)	(n_i^3, m_i^3)
$N_a = 3$	$(n_a^1, \epsilon \tilde{\epsilon} \beta^1)$	$(3, \frac{1}{2} \tilde{\epsilon} \epsilon)$	1_3
$N_b = 2$	$(1/\beta_1, 0)$	$(1, \frac{1}{2} \epsilon \tilde{\epsilon})$	$\alpha^2 \mathbf{1}_2$
$N_c = 1$	$(1/\beta_1, 0)$	$(0, -\epsilon \tilde{\epsilon})$	α^2
$N_d = 1$	$(n_d^1, 3\epsilon \beta^1)$	$(\tilde{\epsilon}, -\frac{1}{2} \epsilon)$	1
N_h	$(\epsilon_h/\beta^1, 0)$	$(2, 0)$	1_{N_h}

Table 7: General tadpole solutions for the four-stack Q2-type quiver of intersecting D5-branes, giving rise to exactly the standard model gauge group and observable chiral spectrum at low energies. The solutions depend on two integer parameters, n_a^1 , n_d^1 , the NS-background β^1 and the phase parameters $\epsilon = \tilde{\epsilon} = \pm 1$, as well as the CP phase α .

The solutions satisfying simultaneously the intersection constraints and the cancellation of the RR twisted crosscap tadpole cancellation constraints are given in parametric form in table (7). These solutions represent the most general solution of the RR tadpoles. The solutions of table (7) satisfy all RR tadpole cancellation conditions

in (2.16) but the first. The latter reads :

$$9n_a^1 - \frac{1}{\beta^1} + n_d^1 \tilde{\epsilon} + \frac{2\epsilon_h N_h}{\beta^1} = -8. \quad (4.15)$$

In this case the $U(1)$ couplings to twisted RR fields read

$$\begin{aligned} B_2^{(1)} &\wedge c_1 \left[2 \frac{(\alpha^2 - \alpha)}{\beta^1} \right] F^b, \\ D_2^{(1)} &\wedge c_1 [\epsilon \tilde{\epsilon}] \left[3n_a^1 F^a - \frac{1}{\beta^1} F^b + \frac{1}{\beta^1} F^c - \tilde{\epsilon} n_d^1 F^d \right], \\ E_2^{(1)} &\wedge c_1 [6\epsilon \tilde{\epsilon} \beta^1] [3F^a + F^d]. \end{aligned} \quad (4.16)$$

The combination of the $U(1)$'s

$$Q^l = (Q_a - 3Q_d) - 3\beta^1 (n_a^1 + \tilde{\epsilon} n_d^1) Q_c. \quad (4.17)$$

represents the hypercharge if the condition

$$\beta^1 (n_a^1 + \tilde{\epsilon} n_d^1) = 1 \quad (4.18)$$

is satisfied.

An alternative RR tadpole solution for the Q2-quiver class of SM's can be seen in table (8).

N_i	(n_i^1, m_i^1)	(n_i^2, m_i^2)	(n_i^3, m_i^3)
$N_a = 3$	$(n_a^1, -\epsilon \tilde{\epsilon} \beta^1)$	$(3, -\frac{1}{2} \tilde{\epsilon} \epsilon)$	1_3
$N_b = 2$	$(1/\beta^1, 0)$	$(1, -\frac{1}{2} \epsilon \tilde{\epsilon})$	$\alpha^2 1_2$
$N_c = 1$	$(1/\beta^1, 0)$	$(0, -\epsilon \tilde{\epsilon})$	α^2
$N_d = 1$	$(n_d^1, 3\epsilon \beta^1)$	$(-\tilde{\epsilon}, -\frac{1}{2} \epsilon)$	1
N_h	$(\epsilon_h/\beta^1, 0)$	$(2, 0)$	1_{N_h}

Table 8: Alternative general tadpole solutions for the four-stack Q2-type quiver of intersecting D5-branes, giving rise to exactly the standard model gauge group and observable chiral spectrum at low energies. The solutions depend on two integer parameters, n_a^1 , n_d^1 , the NS-background β^1 and the phase parameters $\epsilon = \tilde{\epsilon} = \pm 1$, as well as the CP phase α .

In this case the $U(1)$ couplings to twisted RR fields read

$$\begin{aligned}
B_2^{(1)} &\wedge c_1[2\frac{(\alpha^2 - \alpha)}{\beta^1}]F^b, \\
D_2^{(1)} &\wedge c_1[\epsilon\tilde{\epsilon}][-3n_a^1 F^a + \frac{1}{\beta^1} F^b + \frac{1}{\beta^1} F^c - \tilde{\epsilon}n_d^1 F^d], \\
E_2^{(1)} &\wedge c_1[-6\epsilon\epsilon\beta^1][3F^a + F^d].
\end{aligned} \tag{4.19}$$

The solutions of table (8) satisfy all RR tadpole cancellation conditions in (2.16) but the first. The latter being

$$9n_a^1 - \frac{1}{\beta^1} + n_d^1\tilde{\epsilon} + \frac{2\epsilon_h N_h}{\beta^1} = -8. \tag{4.20}$$

The $U(1)$ which remains massless reads

$$Q^l = (Q_a - 3Q_d) + 3\beta^1(n_a^1 - \tilde{\epsilon}n_d^1)Q_c. \tag{4.21}$$

The latter $U(1)$ is the SM hypercharge if

$$\beta^1(n_a^1 - \tilde{\epsilon}n_d^1) = -1. \tag{4.22}$$

4.4 Scalar sector of the ‘reflected’ Q2-quiver

We will make the choice of RR tadpole parameters by taking into account the constraints (4.15), (4.18). We choose

$$n_a^1 = 1, \quad n_d^1 = 1, \quad \beta^1 = 1/2, \quad \epsilon_h = -1, \quad N_h = 4, \quad \epsilon = 1, \quad \tilde{\epsilon} = 1 \tag{4.23}$$

Sector	Representation	$\alpha' \cdot mass^2$
aa^*	$2(3, 1)_{1/3} + (6, 1)_{-1/3}$	0
ad	$2(3, 1)_{-2/3}$	0
ad^*	$2(3, 1)_{1/3}$	$\pm \frac{1}{\pi} \tan^{-1} \left(\frac{U^2}{2} \right)$

Table 9: Lightest scalar excitations for the four stack Q2-quiver SM’s. The limit $U^1 = (U^2)/3$ is taken.

By choosing $U^1 = U^2/3$ the mass of the colour aa^* , ad sector singlets goes to zero while the scalars from the ad^* -sectors have a tachyonic direction. The latter should be lifted by loop corrections as it has been emphasized before(see also (5.3)). Thus at low energies only the SM should remain.

4.5 SM vacua from the ‘reflected’ Q3-Quiver

In this subsection we examine the derivation of exactly the SM at low energies from the embedding of the four stack SM structure of table (1) in a Z_3 quiver of $Q3$ -type.

N_i	(n_i^1, m_i^1)	(n_i^2, m_i^2)	(n_i^3, m_i^3)
$N_a = 3$	$(1/\beta_1, 0)$	$(1, \frac{1}{2}\tilde{\epsilon}\epsilon)$	$\alpha^2 1_3$
$N_b = 2$	$(n_b^1, \tilde{\epsilon}\epsilon\beta^1)$	$(1, \frac{3}{2}\epsilon\tilde{\epsilon})$	1_2
$N_c = 1$	$(n_c^1, 3\epsilon\beta^1)$	$(0, -\epsilon)$	1
$N_d = 1$	$(1/\beta_1, 0)$	$(-1, \frac{3}{2}\epsilon\tilde{\epsilon})$	α
N_h	$(\epsilon_h/\beta^1, 0)$	$(2, 0)$	1_{N_h}

Table 10: General tadpole solutions for the four-stack $Q3$ -type quiver of intersecting D5-branes, giving rise to models, with exactly the standard model gauge group and observable chiral spectrum at low energies. The solutions depend on two integer parameters, n_b^1, n_c^1 , the NS-background β^1 and the phase parameters $\epsilon = \tilde{\epsilon} = \pm 1$, as well as the CP phase α .

The solutions satisfying simultaneously the intersection constraints and the cancellation of the RR twisted crosscap tadpole cancellation constraints are given in parametric form in table (10). The solutions of table (10) satisfy all tadpole equations in (2.16) but the first. The latter reads :

$$n_b^1 = -4 + \frac{1}{2\beta^1}(1 - 2\epsilon_h N_h). \quad (4.24)$$

Also in this case the $U(1)$ couplings to twisted RR fields read

$$\begin{aligned} B_2^{(1)} \wedge c_1\left[\frac{(\alpha^2 - \alpha)}{\beta^1}\right][3F^a + F^d], \\ D_2^{(1)} \wedge c_1[\epsilon\tilde{\epsilon}]\left[-\frac{3}{2\beta^1}F^a + 6n_b^1 F^b - 2n_c^1 \tilde{\epsilon}F^c - \frac{3}{2\beta^1}F^d\right], \\ E_2^{(1)} \wedge c_1[4\epsilon\tilde{\epsilon}\beta^1]F^b. \end{aligned} \quad (4.25)$$

The low energy $U(1)$ combination

$$Q^l = (Q_a - 3Q_d) + \frac{3\epsilon}{2\beta^1 n_c^1} Q_c. \quad (4.26)$$

is the hypercharge if

$$n_c^1 = -\frac{\epsilon}{2\beta^1} . \quad (4.27)$$

From (4.24), (4.27) we conclude that $\beta^1 = 1/2$.

An alternative RR tadpole cancellation to the one appearing in table (10) appears in table (11).

N_i	(n_i^1, m_i^1)	(n_i^2, m_i^2)	(n_i^3, m_i^3)
$N_a = 3$	$(1/\beta_1, 0)$	$(1, -\frac{1}{2}\tilde{\epsilon}\epsilon)$	$\alpha^2 1_3$
$N_b = 2$	$(n_b^1, -\tilde{\epsilon}\epsilon\beta^1)$	$(1, -\frac{3}{2}\epsilon\tilde{\epsilon})$	$\mathbf{1}_2$
$N_c = 1$	$(n_c^1, 3\epsilon\beta^1)$	$(0, -\epsilon)$	1
$N_d = 1$	$(1/\beta_1, 0)$	$(-1, -\frac{3}{2}\epsilon\tilde{\epsilon})$	α
N_h	$(\epsilon_h/\beta^1, 0)$	$(2, 0)$	1_{N_h}

Table 11: Alternative general tadpole solutions for the four-stack $Q3$ -type quiver of intersecting D5-branes, giving rise to models with exactly the standard model gauge group and observable chiral spectrum at low energies. The solutions depend on two integer parameters, n_b^1, n_c^1 , the NS-background β^1 and the phase parameters $\epsilon = \tilde{\epsilon} = \pm 1$, as well as the CP phase α .

In this case, all tadpole conditions but the first, in (2.16), are satisfied, thus

$$n_b^1 = -4 + \frac{1}{2\beta^1}(1 - 2\epsilon_h N_h) \quad (4.28)$$

The $U(1)$ couplings to twisted RR fields read:

$$\begin{aligned}
B_2^{(1)} \wedge c_1 \left[\frac{(\alpha^2 - \alpha)}{\beta^1} \right] [3F^a + F^d], \\
D_2^{(1)} \wedge c_1 [\epsilon\tilde{\epsilon}] \left[\frac{3}{2\beta^1} F^a - 6n_b^1 F^b - 2n_c^1 \tilde{\epsilon} F^c + \frac{3}{2\beta^1} F^d \right], \\
E_2^{(1)} \wedge c_1 [-4\epsilon\tilde{\epsilon}\beta^1] F^b.
\end{aligned} \quad (4.29)$$

In this case, the combination of the $U(1)$'s which is the SM hypercharge is

$$Q^l = (Q_a - 3Q_d) - \frac{3\tilde{\epsilon}}{2\beta^1 n_c^1} Q_c. \quad (4.30)$$

if the hypercharge condition is satisfied, namely

$$n_c^1 = \frac{\tilde{\epsilon}}{2\beta^1} \quad (4.31)$$

From (4.28), (4.31) we conclude that $\beta^1 = 1/2$.

4.6 Scalar sector of the ‘reflected’ Q3-quiver

We will make the choice of RR tadpole parameters by taking into account the constraints (4.15), (4.18). We choose

$$n_b^1 = 1, \quad n_c^1 = 1, \quad \beta^1 = 1/2, \quad \epsilon_h = -1, \quad N_h = 4, \quad \epsilon = -1, \quad \tilde{\epsilon} = -1 \quad (4.32)$$

Sector	Representation	$\alpha' \cdot mass^2$
bb^*	$3(1, 1)_0$	$\pm \frac{1}{\pi} [\tan^{-1}(\frac{U^1}{2}) - \tan^{-1}(\frac{U^2}{2})]$
bc	$2(2, 1)_{1/2}$	$\pm \frac{1}{2\pi} [\tan^{-1}(\frac{U^1}{2}) + \tan^{-1}(\frac{3U^1}{2}) - \tan^{-1}(\frac{3U^2}{2}) + \tan^{-1}(\frac{U^2}{0})]$
bc^*	$(2, 1)_{-1/2}$	$\pm \frac{1}{\pi} [\tan^{-1}(\frac{U^1}{2}) - \tan^{-1}(\frac{3U^1}{2}) - \tan^{-1}(\frac{3U^2}{2}) + \tan^{-1}(\frac{U^2}{0})]$

Table 12: Lightest scalar excitations for the four stack Q3-quiver SM’s.

If we choose $U^1 = U^2$ then the mass of the aa^* scalars goes to zero. However the scalars from the bc , bc^* may tend to zero only when the U^1 modulus assumes simultaneously the limit $U^1 \rightarrow \infty$, a decompactification limit. However, it is possible to lift these tachyonic directions by loop corrections [6, 2], that are not expected to be so strong as for colour scalars. Thus the SM may remain at low energies. An alternative way to show that there always be directions in the moduli space that will give the SM at low energy will be shown in section 7 using brane recombination.

4.7 SM vacua from the ‘reflected’ Q4-Quiver

In this subsection we examine the derivation of exactly the SM at low energies from the embedding of the four stack SM structure of table (1) in a Z_3 quiver of Q4-type.

The solutions satisfying simultaneously the intersection constraints and the cancellation of the RR twisted crosscap tadpole cancellation constraints are given in parametric form in table (13). These solutions represent the most general solution of the

N_i	(n_i^1, m_i^1)	(n_i^2, m_i^2)	(n_i^3, m_i^3)
$N_a = 3$	$(1/\beta_1, 0)$	$(1, \frac{1}{2}\tilde{\epsilon}\epsilon)$	$\alpha^2 1_3$
$N_b = 2$	$(n_b^1, \tilde{\epsilon}\epsilon\beta^1)$	$(1, \frac{3}{2}\epsilon\tilde{\epsilon})$	$\mathbf{1}_2$
$N_c = 1$	$(n_c^1, 3\epsilon\beta^1)$	$(0, -\epsilon)$	1
$N_d = 1$	$(1/\beta_1, 0)$	$(1, -\frac{3}{2}\epsilon\tilde{\epsilon})$	α^2
N_h	$(\epsilon_h/\beta^1, 0)$	$(2, 0)$	1_{N_h}

Table 13: General tadpole solutions for the four-stack $Q4$ -type quiver of intersecting D5-branes, giving rise to models with exactly the standard model gauge group and observable chiral spectrum at low energies. The solutions depend on two integer parameters, n_b^1 , n_c^1 , the NS-background β^1 and the phase parameters $\epsilon = \tilde{\epsilon} = \pm 1$, as well as the CP phase α .

twisted RR tadpoles (2.16). The solutions of table (13) satisfy all tadpole equations, in (2.16), but the first. The latter reads :

$$n_b^1 = -4 + \frac{1}{\beta^1}(1 - \epsilon_h N_h). \quad (4.33)$$

Further, the $U(1)$ couplings to twisted RR fields read

$$\begin{aligned}
B_2^{(1)} \wedge c_1 \left[\frac{(\alpha^2 - \alpha)}{\beta^1} \right] [3F^a + F^d], \\
D_2^{(1)} \wedge c_1 [\epsilon\tilde{\epsilon}] \left[-\frac{3}{2\beta^1} F^a + 6n_b^1 F^b - 2n_c^1 \tilde{\epsilon} F^c + \frac{3}{2\beta^1} F^d \right], \\
E_2^{(1)} \wedge c_1 [4\epsilon\tilde{\epsilon}\beta^1] F^b.
\end{aligned} \quad (4.34)$$

The ‘light’ $U(1)$ combination

$$Q^l = (Q_a - 3Q_d) - \frac{3\epsilon}{\beta^1 n_c^1} Q_c. \quad (4.35)$$

is identified as the SM hypercharge if the condition

$$n_c^1 = \frac{\epsilon}{\beta^1} \quad (4.36)$$

is satisfied. From (4.33), (4.36) we conclude that $\beta^1 = 1$.

An alternative RR tadpole cancellation to the one appearing in table (13) appears in table (14). The twisted RR solutions of table (14) satisfy all tadpole equations, in

N_i	(n_i^1, m_i^1)	(n_i^2, m_i^2)	(n_i^3, m_i^3)
$N_a = 3$	$(1/\beta_1, 0)$	$(1, -\frac{1}{2}\tilde{\epsilon}\epsilon)$	$\alpha^2 1_3$
$N_b = 2$	$(n_b^1, -\tilde{\epsilon}\epsilon\beta^1)$	$(1, -\frac{3}{2}\epsilon\tilde{\epsilon})$	1_2
$N_c = 1$	$(n_c^1, 3\epsilon\beta^1)$	$(0, -\epsilon)$	1
$N_d = 1$	$(1/\beta_1, 0)$	$(1, \frac{3}{2}\epsilon\tilde{\epsilon})$	α^2
N_h	$(\epsilon_h/\beta^1, 0)$	$(2, 0)$	1_{N_h}

Table 14: Alternative general tadpole solutions for the four-stack $Q4$ -type quiver of intersecting D5-branes, giving rise to SM-like models with exactly the standard model gauge group and observable chiral spectrum at low energies and also some scalars. The solutions depend on two integer parameters, n_b^1, n_c^1 , the NS-background β^1 and the phase parameters $\epsilon = \tilde{\epsilon} = \pm 1$, as well as the CP phase α .

(2.16), but the first. The latter reads :

$$n_b^1 = -4 + \frac{1}{\beta^1}(1 - \epsilon_h N_h). \quad (4.37)$$

In this case the $U(1)$ couplings to twisted RR fields read

$$\begin{aligned}
B_2^{(1)} \wedge c_1\left[\frac{(\alpha^2 - \alpha)}{\beta^1}\right][3F^a + F^d], \\
D_2^{(1)} \wedge c_1[\epsilon\tilde{\epsilon}]\left[\frac{3}{2\beta^1}F^a - 6n_b^1F^b - 2n_c^1\tilde{\epsilon}F^c - \frac{3}{2\beta^1}F^d\right], \\
E_2^{(1)} \wedge c_1[-4\epsilon\tilde{\epsilon}\beta^1]F^b.
\end{aligned} \quad (4.38)$$

In this alternative solution the $U(1)$ combination

$$Q^l = (Q_a - 3Q_d) + \frac{3\tilde{\epsilon}}{n_c^1\beta^1}Q_c. \quad (4.39)$$

is identified as the hypercharge if

$$n_c^1 = \frac{\tilde{\epsilon}}{\beta^1}. \quad (4.40)$$

From (4.37), (4.40) we conclude that $\beta^1 = 1$. The $Q4$ -models may give the SM at low energy as the scalar tachyonic directions may always be lifted.

4.8 Exact SM vacua from the a1-Quiver

In this subsection we examine the derivation of exactly the SM at low energies from the embedding of the four stack SM structure of table (1) in a Z_3 quiver of $a1$ -type. The latter quiver can be seen in figure (2). For an alternative RR tadpole solution of the $a1$ -quiver see [2].

N_i	(n_i^1, m_i^1)	(n_i^2, m_i^2)	(n_i^3, m_i^3)
$N_a = 3$	$(n_a^1, \tilde{\epsilon}\epsilon\beta^1)$	$(3, -\frac{1}{2}\tilde{\epsilon}\epsilon)$	1_3
$N_b = 2$	$(1/\beta_1, 0)$	$(1, -\frac{1}{2}\epsilon\tilde{\epsilon})$	$\alpha 1_2$
$N_c = 1$	$(1/\beta_1, 0)$	$(0, -\epsilon\tilde{\epsilon})$	α^2
$N_d = 1$	$(n_d^1, 3\epsilon\beta^1)$	$(\tilde{\epsilon}, \frac{1}{2}\epsilon)$	1
N_h	$(\epsilon_h/\beta^1, 0)$	$(2, 0)$	1_{N_h}

Table 15: General tadpole solutions for the four-stack $a1$ -type quiver of intersecting D5-branes, giving rise to exactly the standard model gauge group and observable chiral spectrum at low energies.

The solutions satisfying simultaneously the intersection constraints and the cancellation of the RR twisted crosscap tadpole cancellation constraints are given in parametric form in table (15). These solutions represent the most general solution of the twisted RR tadpoles (2.16). They depend on two integer parameters n_a^1, n_d^1 , the phase parameters $\epsilon = \pm 1, \tilde{\epsilon} = \pm 1$, and the NS-background parameter $\beta_i = 1 - b_i$, which is associated to the presence of the NS B-field by $b_i = 0, 1/2$.

The solutions of table (15) satisfy all tadpole equations, in (2.16), but the first. The latter reads :

$$9n_a^1 - \frac{1}{\beta^1} + \tilde{\epsilon}n_d^1 + \frac{2\epsilon_h N_h}{\beta^1} = -8 \quad (4.41)$$

In this case the $U(1)$ couplings to twisted RR fields read

$$\begin{aligned}
B_2^{(1)} &\wedge c_1 \left[-2 \frac{(\alpha^2 - \alpha)}{\beta^1} \right] F^b, \\
D_2^{(1)} &\wedge c_1 [\epsilon\tilde{\epsilon}] \left[-3n_a^1 F^a + \frac{1}{\beta^1} F^b + \frac{1}{\beta^1} F^c + \tilde{\epsilon}n_d^1 F^d \right], \\
E_2^{(1)} &\wedge c_1 [6\epsilon\tilde{\epsilon}\beta^1] (3F^a + F^d).
\end{aligned} \quad (4.42)$$

From (4.42) it is easily identified the hypercharge as the $U(1)$ combination

$$Q^l = (Q_a - 3Q_d) + 3\beta^1(n_a^1 + \tilde{\epsilon}n_d^1)Q_c. \quad (4.43)$$

which simultaneously satisfies

$$\beta^1(n_a^1 + \tilde{\epsilon}n_d^1) = -1 \quad (4.44)$$

An alternative solution to the RR tadpole solutions for the a1-quiver, we found in table (15), can be seen in table (16).

N_i	(n_i^1, m_i^1)	(n_i^2, m_i^2)	(n_i^3, m_i^3)
$N_a = 3$	$(n_a^1, -\tilde{\epsilon}\epsilon\beta^1)$	$(3, \frac{1}{2}\tilde{\epsilon}\epsilon)$	1_3
$N_b = 2$	$(1/\beta_1, 0)$	$(1, \frac{1}{2}\epsilon\tilde{\epsilon})$	$\alpha 1_2$
$N_c = 1$	$(1/\beta_1, 0)$	$(0, \epsilon\tilde{\epsilon})$	α^2
$N_d = 1$	$(n_d^1, 3\epsilon\beta^1)$	$(-\tilde{\epsilon}, \frac{1}{2}\epsilon)$	1
N_h	$(\epsilon_h/\beta^1, 0)$	$(2, 0)$	1_{N_h}

Table 16: Alternative general twisted RR tadpole solutions for the four-stack a1-type quiver of intersecting D5-branes, giving rise to exactly the standard model gauge group and observable chiral spectrum at low energies. The solutions depend on two integer parameters, n_a^1 , n_d^1 , the NS-background β^1 and the phase parameters $\epsilon = \tilde{\epsilon} = \pm 1$, as well as the CP phase α .

The solutions of table (16) satisfy all tadpole equations, in (2.16), but the first. The latter reads :

$$9n_a^1 - \frac{1}{\beta^1} - \tilde{\epsilon}n_d^1 + \frac{2\epsilon_h N_h}{\beta^1} = -8 \quad (4.45)$$

In this case the $U(1)$ couplings to twisted RR fields read

$$\begin{aligned} B_2^{(1)} &\wedge c_1[2\frac{(\alpha - \alpha^2)}{\beta^1}]F^b, \\ D_2^{(1)} &\wedge c_1[\epsilon\tilde{\epsilon}][3n_a^1 F^a - \frac{1}{\beta^1}F^b - \frac{1}{\beta^1}F^c + \tilde{\epsilon}n_d^1 F^d], \\ E_2^{(1)} &\wedge c_1[-6\epsilon\tilde{\epsilon}\beta^1](3F^a + F^d). \end{aligned} \quad (4.46)$$

Similarly the hypercharge gets identified as the expression

$$Q^l = (Q_a - 3Q_d) + 3\beta^1(n_a^1 - \tilde{\epsilon}n_d^1)Q_c. \quad (4.47)$$

which satisfies the additional condition

$$\beta^1(n_a^1 - \tilde{\epsilon}n_d^1) = -1 \quad (4.48)$$

4.9 Exact SM vacua from the a2-Quiver

In this subsection we examine the derivation of exactly the SM at low energies from the embedding of the four stack SM structure of table (1) in a Z_3 quiver of $a2$ -type. The latter quiver can be seen in figure (2). For an alternative RR tadpole solution of the $a2$ -quiver see [2].

N_i	(n_i^1, m_i^1)	(n_i^2, m_i^2)	(n_i^3, m_i^3)
$N_a = 3$	$(n_a^1, \tilde{\epsilon}\epsilon\beta^1)$	$(3, -\frac{1}{2}\tilde{\epsilon}\epsilon)$	1_3
$N_b = 2$	$(1/\beta_1, 0)$	$(1, -\frac{1}{2}\epsilon\tilde{\epsilon})$	$\alpha 1_2$
$N_c = 1$	$(1/\beta_1, 0)$	$(0, \epsilon\tilde{\epsilon})$	α
$N_d = 1$	$(n_d^1, 3\epsilon\beta^1)$	$(\tilde{\epsilon}, \frac{1}{2}\epsilon)$	1
N_h	$(\epsilon_h/\beta^1, 0)$	$(2, 0)$	1_{N_h}

Table 17: General tadpole solutions for the four-stack $a2$ -type quiver of intersecting D5-branes, giving rise to exactly the standard model gauge group and observable chiral spectrum at low energies.

The solutions satisfying simultaneously the intersection constraints and the cancellation of the RR twisted crosscap tadpole cancellation constraints are given in parametric form in table (17). These solutions represent the most general solution of the twisted RR tadpoles (2.16). They depend on two integer parameters n_a^1, n_d^1 , the phase parameters $\epsilon = \pm 1, \tilde{\epsilon} = \pm 1$, and the NS-background parameter $\beta_i = 1 - b_i$, which is associated to the presence of the NS B-field by $b_i = 0, 1/2$. The solutions of table (17) satisfy all tadpole equations in (2.16), but the first. The latter reads :

$$9n_a^1 - \frac{1}{\beta^1} + \tilde{\epsilon}n_d^1 + \frac{2\epsilon_h N_h}{\beta^1} = -8 \quad (4.49)$$

In this case the $U(1)$ couplings to twisted RR fields read

$$\begin{aligned}
B_2^{(1)} &\wedge c_1[-2\frac{(\alpha^2 - \alpha)}{\beta^1}]F^b, \\
D_2^{(1)} &\wedge c_1[\epsilon\tilde{\epsilon}][-3n_a^1F^a + \frac{1}{\beta^1}F^b - \frac{1}{\beta^1}F^c + \tilde{\epsilon}n_d^1F^d], \\
E_2^{(1)} &\wedge c_1[6\epsilon\tilde{\epsilon}\beta^1](3F^a + F^d).
\end{aligned} \tag{4.50}$$

The combination of the $U(1)$'s

$$Q^l = (Q_a - 3Q_d) - 3\beta^1(n_a^1 + \tilde{\epsilon}n_d^1)Q_c \tag{4.51}$$

may be the SM hypercharge if the condition

$$\beta^1(n_a^1 + \tilde{\epsilon}n_d^1) = 1 \tag{4.52}$$

An alternative solution to the RR tadpole solutions for the a2-quiver, we found in table (17), can be seen in table (18).

N_i	(n_i^1, m_i^1)	(n_i^2, m_i^2)	(n_i^3, m_i^3)
$N_a = 3$	$(n_a^1, -\tilde{\epsilon}\epsilon\beta^1)$	$(3, \frac{1}{2}\tilde{\epsilon}\epsilon)$	1_3
$N_b = 2$	$(1/\beta_1, 0)$	$(1, \frac{1}{2}\epsilon\tilde{\epsilon})$	$\alpha 1_2$
$N_c = 1$	$(1/\beta_1, 0)$	$(0, -\epsilon\tilde{\epsilon})$	α
$N_d = 1$	$(n_d^1, 3\epsilon\beta^1)$	$(-\tilde{\epsilon}, \frac{1}{2}\epsilon)$	1
N_h	$(\epsilon_h/\beta^1, 0)$	$(2, 0)$	1_{N_h}

Table 18: Alternative general twisted RR tadpole solutions for the four-stack a2-type quiver of intersecting D5-branes, giving rise to exactly the standard model gauge group and observable chiral spectrum at low energies. The solutions depend on two integer parameters, n_a^1 , n_d^1 , the NS-background β^1 and the phase parameters $\epsilon = \tilde{\epsilon} = \pm 1$, as well as the CP phase α .

In this case all tadpole equations but the first, in (2.16), are satisfied. The latter reads :

$$9n_a^1 - \frac{1}{\beta^1} - \tilde{\epsilon}n_d^1 + \frac{2\epsilon_h N_h}{\beta^1} = -8 \tag{4.53}$$

In this case the $U(1)$ couplings to twisted RR fields read

$$\begin{aligned}
B_2^{(1)} &\wedge c_1[2\frac{(\alpha - \alpha^2)}{\beta^1}]F^b, \\
D_2^{(1)} &\wedge c_1[\epsilon\tilde{\epsilon}][3n_a^1F^a - \frac{1}{\beta^1}F^b + \frac{1}{\beta^1}F^c + \tilde{\epsilon}n_d^1F^d], \\
E_2^{(1)} &\wedge c_1[-6\epsilon\tilde{\epsilon}\beta^1](3F^a + F^d).
\end{aligned} \tag{4.54}$$

Also in this case, the $U(1)$

$$Q^l = (Q_a - 3Q_d) - 3\beta^1(n_a^1 - \tilde{\epsilon}n_d^1)Q_c \tag{4.55}$$

is being identified as the hypercharge if

$$\beta^1(n_a^1 - \tilde{\epsilon}n_d^1) = 1 \tag{4.56}$$

is satisfied.

4.10 SM vacua from the a3-Quiver

In this subsection we examine the derivation of exactly the SM at low energies from the embedding of the four stack SM structure of table (1) in a Z_3 quiver of $a3$ -type. The latter quiver can be seen in figure (2). For an alternative RR tadpole solution of the $a3$ -quiver see [2].

N_i	(n_i^1, m_i^1)	(n_i^2, m_i^2)	(n_i^3, m_i^3)
$N_a = 3$	$(1/\beta^1, 0)$	$(1, -\frac{1}{2}\tilde{\epsilon}\epsilon)$	$\alpha 1_3$
$N_b = 2$	$(n_b^1, \tilde{\epsilon}\epsilon\beta^1)$	$(1, -\frac{3}{2}\epsilon\tilde{\epsilon})$	$\mathbf{1}_2$
$N_c = 1$	$(n_c^1, 3\epsilon\beta^1)$	$(0, \epsilon)$	1
$N_d = 1$	$(1/\beta^1, 0)$	$(-1, -\frac{3}{2}\epsilon\tilde{\epsilon})$	α^2
N_h	$(\epsilon_h/\beta^1, 0)$	$(2, 0)$	1_{N_h}

Table 19: General twisted RR tadpole solutions for the four-stack $a3$ -type quiver of intersecting D5-branes, giving rise to SM-like models with exactly the standard model gauge group and observable chiral spectrum at low energies.

The solutions satisfying simultaneously the intersection constraints and the cancellation of the RR twisted crosscap tadpole cancellation constraints are given in parametric form in table (19). These solutions represent the most general solution of the twisted RR tadpoles (2.16). They depend on two integer parameters n_b^1, n_c^1 , the phase parameters $\epsilon = \pm 1, \tilde{\epsilon} = \pm 1$, and the NS-background parameter $\beta_i = 1 - b_i$, which is associated to the presence of the NS B-field by $b_i = 0, 1/2$.

The RR tadpole solutions of table (19) satisfy all tadpole equations, in (2.16), but the first. The latter reads :

$$n_b^1 = -4 + \frac{1}{2\beta^1}(1 - 2\epsilon_h N_h) \quad (4.57)$$

In this case the $U(1)$ couplings to twisted RR fields read

$$\begin{aligned} B_2^{(1)} \wedge c_1 \left[\frac{(\alpha - \alpha^2)}{\beta^1} \right] (3F^a + F^d), \\ D_2^{(1)} \wedge c_1 [\epsilon \tilde{\epsilon}] \left[\frac{3}{2\beta^1} F^a - 6n_b^1 F^b + 2n_c^1 \tilde{\epsilon} F^c + \frac{3}{2\beta^1} F^d \right], \\ E_2^{(1)} \wedge c_1 [4\epsilon \tilde{\epsilon} \beta^1] F^b. \end{aligned} \quad (4.58)$$

The $U(1)$ combination given by

$$Q^l = (Q_a - 3Q_d) - \frac{3\tilde{\epsilon}}{2\beta^1 n_c^1} Q_c. \quad (4.59)$$

is the SM hypercharge if

$$n_c^1 = \frac{\tilde{\epsilon}}{2\beta^1} \quad (4.60)$$

From (4.57) and (4.60) we conclude that $\beta^1 = 1/2$.

An alternative solution to the RR tadpole solutions for the a3-quiver, we found in table (19), can be seen in table (20).

The solutions of table (20) satisfy all tadpole equations, in (2.16), but the first. The latter reads :

$$n_b^1 = -4 + \frac{1}{2\beta^1}(1 - 2\epsilon_h N_h) \quad (4.61)$$

In this case the $U(1)$ couplings to twisted RR fields read

$$\begin{aligned} B_2^{(1)} \wedge c_1 \left[\frac{(\alpha - \alpha^2)}{\beta^1} \right] (3F^a + F^d), \\ D_2^{(1)} \wedge c_1 [\epsilon \tilde{\epsilon}] \left[-\frac{3}{2\beta^1} F^a + 6n_b^1 F^b + 2n_c^1 \tilde{\epsilon} F^c - \frac{3}{2\beta^1} F^d \right], \\ E_2^{(1)} \wedge c_1 [-4\epsilon \tilde{\epsilon} \beta^1] F^b. \end{aligned} \quad (4.62)$$

N_i	(n_i^1, m_i^1)	(n_i^2, m_i^2)	(n_i^3, m_i^3)
$N_a = 3$	$(1/\beta^1, 0)$	$(1, \frac{1}{2}\tilde{\epsilon}\epsilon)$	$\alpha 1_3$
$N_b = 2$	$(n_b^1, -\tilde{\epsilon}\epsilon\beta^1)$	$(1, \frac{3}{2}\epsilon\tilde{\epsilon})$	$\mathbf{1}_2$
$N_c = 1$	$(n_c^1, 3\epsilon\beta^1)$	$(0, \epsilon)$	1
$N_d = 1$	$(1/\beta^1, 0)$	$(-1, \frac{3}{2}\epsilon\tilde{\epsilon})$	α^2
N_h	$(\epsilon_h/\beta^1, 0)$	$(2, 0)$	1_{N_h}

Table 20: Alternative general twisted RR tadpole solutions for the four-stack $a3$ -type quiver of intersecting D5-branes, giving rise to models with exactly the standard model gauge group and observable chiral spectrum at low energies and also some scalars. These scalars may always have non-tachyonic mass directions. The solutions depend on two integer parameters, n_b^1, n_c^1 , the NS-background β^1 and the phase parameters $\epsilon = \tilde{\epsilon} = \pm 1$, as well as the CP phase α .

From (4.62) we conclude that the U(1) combination

$$Q^l = (Q_a - 3Q_d) - \frac{3\tilde{\epsilon}}{2\beta^1 n_c^1} Q_c \quad (4.63)$$

is the hypercharge if

$$n_c^1 = \frac{\tilde{\epsilon}}{2\beta^1} \quad (4.64)$$

From (4.61) and (4.64) we conclude that $\beta^1 = 1/2$. That means that the alternative solution of table (20) gives at low energy a SM vacuum with identical parameter as that of (19). Thus there is no need for us to redefine the background to show the equivalence between the two vacua.

4.11 SM vacua from the a4-Quiver

In this subsection we examine the derivation of exactly the SM at low energies from the embedding of the four stack SM structure of table (1) in a Z_3 quiver of $a4$ -type. The latter quiver can be seen in figure (2). For an alternative RR tadpole solution of the $a4$ -quiver see [2].

The solutions satisfying simultaneously the intersection constraints and the cancellation of the RR twisted crosscap tadpole cancellation constraints are given in para-

N_i	(n_i^1, m_i^1)	(n_i^2, m_i^2)	(n_i^3, m_i^3)
$N_a = 3$	$(1/\beta^1, 0)$	$(1, -\frac{1}{2}\tilde{\epsilon}\epsilon)$	$\alpha 1_3$
$N_b = 2$	$(n_b^1, \tilde{\epsilon}\epsilon\beta^1)$	$(1, -\frac{3}{2}\epsilon\tilde{\epsilon})$	$\mathbf{1}_2$
$N_c = 1$	$(n_c^1, 3\epsilon\beta^1)$	$(0, \epsilon)$	1
$N_d = 1$	$(1/\beta^1, 0)$	$(1, \frac{3}{2}\epsilon\tilde{\epsilon})$	α
N_h	$(\epsilon_h/\beta^1, 0)$	$(2, 0)$	1_{N_h}

Table 21: General twisted RR tadpole solutions for the four-stack $a4$ -type quiver of intersecting D5-branes, giving rise to SM models with exactly the standard model gauge group and observable chiral spectrum at low energies. The solutions depend on two integer parameters, n_b^1, n_c^1 , the NS-background β^1 and the phase parameters $\epsilon = \tilde{\epsilon} = \pm 1$, as well as the CP phase α .

metric form in table (21). The solutions of table (21) satisfy all tadpole equations in (2.16), but the first. The latter reads :

$$n_b^1 = -4 + \frac{1}{\beta^1}(1 - \epsilon_h N_h) \quad (4.65)$$

In this case the $U(1)$ couplings to twisted RR fields read

$$\begin{aligned}
B_2^{(1)} \wedge c_1 \left[\frac{(\alpha - \alpha^2)}{\beta^1} \right] (3F^a + F^d), \\
D_2^{(1)} \wedge c_1 [\epsilon\tilde{\epsilon}] \left[-\frac{3}{2\beta^1} F^a + 6n_b^1 F^b + 2n_c^1 \tilde{\epsilon} F^c + \frac{3}{2\beta^1} F^d \right], \\
E_2^{(1)} \wedge c_1 [4\epsilon\tilde{\epsilon}\beta^1] F^b.
\end{aligned} \quad (4.66)$$

From (refrapo3) we conclude that the $U(1)$ combination

$$Q^l = (Q_a - 3Q_d) + \frac{3\tilde{\epsilon}}{\beta^1 n_c^1} Q_c. \quad (4.67)$$

represents the SM hypercharge if the hypercharge condition is satisfied

$$n_c^1 = -\frac{\tilde{\epsilon}}{\beta^1}. \quad (4.68)$$

From (4.65) and (4.68) we conclude that $\beta^1 = 1$.

An alternative solution to the RR tadpole solutions for the $a4$ -quiver can be seen in table (22).

N_i	(n_i^1, m_i^1)	(n_i^2, m_i^2)	(n_i^3, m_i^3)
$N_a = 3$	$(1/\beta^1, 0)$	$(1, \frac{1}{2}\tilde{\epsilon}\epsilon)$	$\alpha 1_3$
$N_b = 2$	$(n_b^1, -\tilde{\epsilon}\epsilon\beta^1)$	$(1, \frac{3}{2}\epsilon\tilde{\epsilon})$	$\mathbf{1}_2$
$N_c = 1$	$(n_c^1, 3\epsilon\beta^1)$	$(0, \epsilon)$	1
$N_d = 1$	$(1/\beta^1, 0)$	$(1, -\frac{3}{2}\epsilon\tilde{\epsilon})$	α
N_h	$(\epsilon_h/\beta^1, 0)$	$(2, 0)$	1_{N_h}

Table 22: Alternative general twisted RR tadpole solutions for the four-stack $a4$ -type quiver of intersecting D5-branes, giving rise to models with the standard model gauge group and observable chiral spectrum at low energies and also some tachyons scalars. The tachyon directions may always be lifted to positive values. The solutions depend on two integer parameters, n_b^1 , n_c^1 , the NS-background β^1 and the phase parameters $\epsilon = \tilde{\epsilon} = \pm 1$, as well as the CP phase α .

The solutions of table (22) satisfy all tadpole equations in (2.16), but the first. The latter reads :

$$n_b^1 = -4 + \frac{1}{\beta^1}(1 - \epsilon_h N_h) \quad (4.69)$$

In this case the $U(1)$ couplings to twisted RR fields read

$$\begin{aligned}
B_2^{(1)} \wedge c_1 \left[\frac{(\alpha - \alpha^2)}{\beta^1} \right] (3F^a + F^d), \\
D_2^{(1)} \wedge c_1 [\epsilon\tilde{\epsilon}] \left[-\frac{3}{2\beta^1} F^a + 6n_b^1 F^b + 2n_c^1 \tilde{\epsilon} F^c + \frac{3}{2\beta^1} F^d \right], \\
E_2^{(1)} \wedge c_1 [4\epsilon\tilde{\epsilon}\beta^1] F^b.
\end{aligned} \quad (4.70)$$

The combination of the $U(1)$'s which remains light at low energies is identical to (4.67). Also the hypercharge condition in this case is identical to (4.68). In addition $\beta^1 = 1$.

4.12 Effective SM Theories from the Qi and ai Quivers

As we have already pointed out the theories described by the Qi -, ai -quivers, $i = 1, \dots, 4$, and seen in figures (1), (2), are in one to one correspondence. Lets us show that the theories described by these quivers are equivalent. The correspondence is

$$a_1 \Leftrightarrow Q_1, \quad a_2 \Leftrightarrow Q_2, \quad a_3 \Leftrightarrow Q_3, \quad a_4 \Leftrightarrow Q_4, \quad (4.71)$$

Lets us discuss the relation $a_1 \Leftrightarrow Q_1$. A direct comparison of the theories between the two quivers, e.g. using the relations (4.2), (4.8), (4.9) for the Q1-quiver and (4.41), (4.43), (4.44) for the a1-quiver, shows that the first tadpole condition, and the hypercharge of the initially different classes of models are identical ¹⁰. That means that the low energy content of the the two quivers is identical as matter as it concerns the fermion sector; the low energy effective theories are identical. For the two classes of theories to be actually equivalent we have to show that their scalar sector as well the couplings of the antisymmetric fields to various two form RR fields are identical. This is obvious, since the data that we have to take into account to calculate the scalar sector are based on the selection of a particular set of wrapping numbers satisfying the first tadpole condition and the hypercharge condition. The latter equations are identical, thus the scalar sector is identical for both theories. Also the various couplings to twisted RR fields are the same. In the following, we compare the theories coming from their general RR tadpole solutions and not their alternative solutions seen in tables (8), (10), (12), (16), (18), (20).

Identical relations hold for the other pair $a_2 \Leftrightarrow Q_2$.

For the pair $a_3 \Leftrightarrow Q_3$ we need to transform

$$\epsilon \xrightarrow{Q_3 \rightarrow a_3} \tilde{\epsilon}, \quad (4.72)$$

in the Q_3 quiver relations to show that the two class of SM theories are identical.

For the pair $a_4 \Leftrightarrow Q_4$ we need to transform

$$\epsilon \xrightarrow{Q_4 \rightarrow a_4} -\tilde{\epsilon}, \quad (4.73)$$

in the Q_4 quiver relations to show that the two class of SM theories are identical. We note that the correspondence between the ‘reflected’ quivers Q_i and their ‘images’ ai is most easily seen in the solutions presented in this work.

Alternatively, we could try to prove the equivalence e.g. of the effective theories for the Q_i -quivers presented in this work and those one’s that follow from the RR tadpole solutions for the ai -quivers, that appeared in [2]. In this case the transformations needed for the two theories to be proven equivalent are more complicated, as can be seen by the field redefinition,

$$\beta^1 \xrightarrow{Q_2 \rightarrow 4.a_1} \tilde{\epsilon} \beta^1, \quad \tilde{\epsilon} n_d^1 \xrightarrow{Q_1 \rightarrow 4.a_1} n_d^1. \quad (4.74)$$

We note that we have used the RR tadpole solutions of the 4. a_1 -quiver (the a2-quiver

¹⁰Also identical appear to be the couplings to RR fields

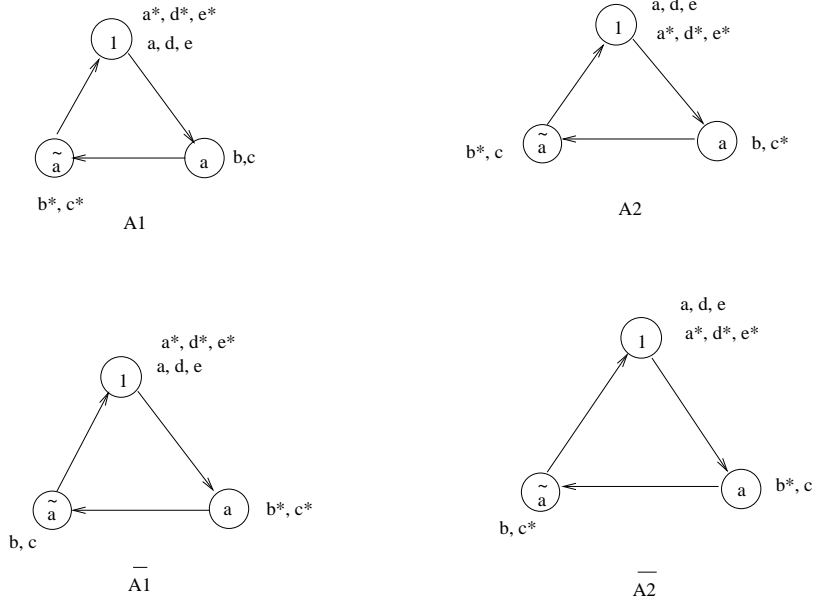


Figure 3: Assignment of SM embedding in configurations of five stacks of D5 branes depicted by Z_3 quiver diagrams. At low energy we get the SM. Note that $\tilde{\alpha} = \alpha^{-1}$.

of the present work) of [2] and also relations (4.49), (4.50), (4.51), (4.52), of the present work.

5 Standard Model Vacua from Five-Stack Quivers

In this chapter, we will discuss the basic elements of the five stack SM quiver embedding classification, namely the classification of the different quivers describing the SM embedding of chiral fermions of different intersecting D5 branes that appear in table (2). We discuss for simplicity the embedding in Z_3 quivers. For each class of models, we present the general class of solutions to the twisted RR tadpole solutions, the two massless $U(1)$'s, surviving the Green-Schwarz mechanism, as well the hypercharge condition on the parameters of the tadpole solutions, that is needed for one of the massless $U(1)$'s to be identified with the hypercharge generator of the SM. We will explicitly describe the scalars generically present in the models only for the A_1 (B1 in appendix) quiver. The scalars generically present in these classes of models are expected to get massive from the loop corrections (5.18). Also, the extra, beyond the hypercharge combination, anomaly free $U(1)$'s get massive by the use of the some charged scalars getting a vev and/or their non-zero coupling to twisted RR fields. Thus in the classes of

theories coming from five stack quivers, the SM survives in general down to low energy. In general one expects to find always tachyonic scalars that might look problematic. However, the tachyonic directions might be lifted by loop corrections (see section (5.3)) or as we will show in section 7, the present SM-like structure of the models is not permanent as using brane recombination the models flow to the associated four stack quiver ¹¹. In this procedure we have assumed that brane recombination e.g. $d + e \rightarrow \tilde{d}$ takes place .

The multiparameter tadpole solutions appearing in tables (23), (25), (26), (27), represent deformations of the D5-brane branes, of table (2), intersecting at angles, within the same homology class of the factorizable two-cycles.

5.1 SM Vacua from the Five-Stack A1-type quiver

The first class of models, that give the SM at low energy, are associated with the A1-quiver and can be seen in figure (3).

N_i	(n_i^1, m_i^1)	(n_i^2, m_i^2)	(n_i^3, m_i^3)
$N_a = 3$	$(n_a^1, -\epsilon\beta^1)$	$(3, \frac{1}{2}\tilde{\epsilon}\epsilon)$	1_3
$N_b = 2$	$(1/\beta_1, 0)$	$(\tilde{\epsilon}, \frac{1}{2}\epsilon)$	$\alpha 1_2$
$N_c = 1$	$(1/\beta_1, 0)$	$(0, -\epsilon)$	α
$N_d = 1$	$(n_d^1, -2\epsilon\beta^1)$	$(1, -\frac{1}{2}\epsilon\tilde{\epsilon})$	1
$N_e = 1$	$(n_e^1, -\epsilon\beta^1)$	$(1, -\frac{1}{2}\epsilon\tilde{\epsilon})$	1
N_h	$(\epsilon_h/\beta^1, 0)$	$(2, 0)$	1_{N_h}

Table 23: General tadpole solutions for the five-stack A1-type quiver of intersecting D5-branes, giving rise to SM at low energies. The solutions depend on three integer parameters, n_a^1, n_d^1, n_e^1 , the NS-background β^1 and the phase parameters $\epsilon = \tilde{\epsilon} = \pm 1$, as well as the CP phase α .

The solutions satisfying simultaneously the intersection constraints and the cancellation of the RR crosscap tadpole constraints are given in parametric form in table

¹¹which is obtained by naively deleting the e-brane from the five stack quiver

(23). These solutions represent the most general solution of the twisted RR tadpoles.

The solutions of table (23) satisfy all tadpole equations in (2.16), but the first. The latter becomes :

$$9n_a^1 - \frac{\tilde{\epsilon}}{\beta^1} + n_d^1 + n_e^1 + \frac{2\epsilon_h N_h}{\beta^1} = -8 \quad (5.1)$$

Note that we had added the presence of extra N_h branes. Their contribution to the RR tadpole conditions is best described by placing them in the three-factorizable cycle

$$N_h \ (\epsilon_h/\beta_1, 0) \ (2, 0) 1_{N_h} \quad (5.2)$$

The presence of N_h D5-branes, give an extra $U(N_h)$ gauge group, which don't contribute to the rest of the tadpoles and intersection constraints. Thus in terms of the low energy theory their presence has no effect. For the A1-quiver the constraints from $U(1)$ anomaly cancellation appear into three terms

$$\begin{aligned} B_2^{(1)} \wedge c_1 \left(\frac{2\tilde{\epsilon}(\alpha - \alpha^2)}{\beta^1} \right) F^b, \\ D_2^{(1)} \wedge c_1 \left(\epsilon\bar{\epsilon}(3n_a^1 F^a - n_d^1 F^d - n_e^1 F^e) - \frac{\epsilon}{\beta^1}(F^b - F^c) \right), \\ E_2^{(1)} \wedge c_1 [-2\epsilon\beta^1][9F^a + 2F^d + F^e]. \end{aligned} \quad (5.3)$$

A $U(1)$, which is orthogonal to the $U(1)$'s coupled to the RR fields in (5.3), is given by

$$Q^l = (Q_a - 3Q_d - 3Q_e) - 3\tilde{\epsilon}\beta^1(n_a^1 + n_d^1 + n_e^1)Q_c. \quad (5.4)$$

The subclass of tadpole solutions of (5.4) having the SM hypercharge assignment at low energies is exactly the one which is proportional to (3.5). It satisfies the condition,

$$\tilde{\epsilon}\beta_1 (n_a^1 + n_d^1 + n_e^1) = 1. \quad (5.5)$$

Summarizing, as long as (5.5) holds (5.4) is the hypercharge generator of the SM. Thus at low energies we get the chiral fermion content of the SM that gets localized according to open string sectors appearing in table (2). We note that there is one extra anomaly free $U(1)$ beyond the hypercharge combination which is

$$Q^{(5)} = Q_d - 2Q_e + Q_c \quad (5.6)$$

The latter $U(1)$ is orthogonal to the $U(1)$'s seen in (5.3), if

$$-n_d^1 + 2n_e^1 + \frac{\tilde{\epsilon}}{\beta_1} = 0 \quad (5.7)$$

The following choice of wrapping numbers is consistent with the constraints (5.1), (5.5), (5.7)

$$\beta_1 = 1, \quad n_d^1 = 3, \quad n_e^1 = 1, \quad n_a^1 = -3, \quad \tilde{\epsilon} = 1, \quad \epsilon = 1, \quad \epsilon_h = -1, \quad N_h = 8 \quad (5.8)$$

One comment is in order. The A1-quiver five stack diagram is similar to the a2-four stack quiver of table (2). Their only difference stems from the addition of the 5-th stack of e -branes in the quiver node which transforms with CP phase **1**. By taking the limit of vanishing e brane, at the same time taking the limit where the contributions of the e -brane to the hypercharge generator vanish, e.g. $n_e^1 \rightarrow 0$, we recover the corresponding four stack hypercharge that is associated with the a2-quiver in (4.43) only if the moduli tadpole parameters of the five stack A1-quiver SM-like model change as follows:

$$\tilde{\epsilon}\beta^1 \rightarrow \beta^1, \quad n_d^1 \rightarrow \tilde{\epsilon}n_d^1, \quad \epsilon_h \rightarrow \frac{\epsilon_h}{\tilde{\epsilon}}. \quad (5.9)$$

Thus quivers on different stacks appear to have the same effective low energy theory, the SM, at low energy. Actually, the tadpole constraint at the limit $n_e^1 = 0$ are the same for both theories (see (5.1), (4.49)). However, it appears at this stage that their scalar sectors are not identical. It will not be the case. Later in section 7 we will see that all five stack quivers are identical theories to their associated four stack quivers thus they have only the SM at low energy, also suggesting that string vacua in the present models are continuously connected.

5.2 Higgs sector of the Five-Stack A1-quiver

A general comment is in order.

The A1 five-stack quiver describes the embedding of the SM chiral fermions of table 2, in the A1-quiver. However, all quivers described in this work, are constructed by deforming around the QCD intersections I_{ab} , I_{ab^*} , I_{ac} , I_{ac^*} . Thus the Higgs sector which is coming from b, c , branes is of common origin to the present D5-branes and also in the corresponding five-stack D6 models of [33]. This is easily understood as it is the SM embedding of table 2 which is embedded in either the present D5-brane models or the D6-brane models of [33]. For the sake of completeness we will repeat some aspects of this mechanism.

The set of Higgs present in the models get localized on the bc , bc^* intersections. The Higgs available in the models can be seen in [33] Apriori, this set of Higgs, are part of the massive spectrum of fields localized in the intersections bc, bc^* . However, the Higgses H_i , h_i become massless, and effectively tachyonic triggering electroweak symmetry breaking, by varying the distance along the first tori between the b, c^* , b, c

branes respectively. Similar set of Higgs fields appear in the four [32], five [33], six stack $D6$ -SM's [34] as well the Pati-Salam four stack $D6$ -models [35].

For the models presented in this work, the number of complex scalar doublets is equal to the non-zero intersection number product between the bc , bc^* branes in the second complex plane. As it have been discussed before in [32, 33, 34, 35] the presence of scalar doublets H^\pm, h^\pm , can be seen as coming from a field theory mass matrix involving the fields H_i and h_i defined as

$$H^\pm = \frac{1}{2}(H_1^* \pm H_2); \quad h^\pm = \frac{1}{2}(h_1^* \pm h_2) . \quad (5.10)$$

and making the effective potential which corresponds to the spectrum of Higgs scalars to be given by

$$\begin{aligned} V_{Higgs} = & m_H^2(|H_1|^2 + |H_2|^2) + m_h^2(|h_1|^2 + |h_2|^2) \\ & + m_B^2 H_1 H_2 + m_b^2 h_1 h_2 + h.c., \end{aligned} \quad (5.11)$$

where

$$\begin{aligned} m_h^2 &= \frac{M_s^2 Z_1^{(bc)}}{4\pi^2} \quad ; \quad m_H^2 = \frac{M_s^2 Z_1^{(bc^*)}}{4\pi^2} \\ m_b^2 &= \frac{M_s^2}{2\alpha'} |\vartheta_2^{(bc)}| \quad ; \quad m_B^2 = \frac{M_s^2}{2\alpha'} |\vartheta_2^{(bc^*)}|, \end{aligned} \quad (5.12)$$

where

$$\vartheta_2^{(bc)} = \frac{\pi}{2} + \tan^{-1} \left(\frac{U^2}{2} \right), \quad \vartheta_2^{(bc^*)} = \frac{\pi}{2} - \tan^{-1} \left(\frac{U^2}{2} \right), \quad (5.13)$$

and we have made the choice of parameters (5.8).

We note that the Z_1 is a free parameter, a moduli, and thus can become very small in relation to the Planck scale.

5.3 Scalar sectors of the Five-Stack A1-quiver

Scalars appear in the theory in sectors that share the same CP phase. Thus for example in the A1-quiver that we will examine in detail, the lightest scalars appear from the nine intersections aa^* , dd^* , ee^* , ad , ad^* , ae , ae^* , de , de^* . They are listed in table (24). We note that the subscript in the scalar representations denotes the hypercharge.

Let us make the choice (5.8). Within this choice, the angles that the branes a , b , c , d , e form with the orientifold plane appear as follows :

$$\vartheta_a^1 = -\pi + \tan^{-1} \left(\frac{U^1}{5} \right), \quad \vartheta_d^1 = -\tan^{-1} \left(\frac{2U^1}{3} \right), \quad (5.14)$$

$$\vartheta_a^2 = -\tan^{-1}\left(\frac{U^2}{6}\right), \quad \vartheta_d^2 = \tan^{-1}\left(\frac{U^2}{2}\right), \quad (5.15)$$

$$\vartheta_e^1 = -\tan^{-1}\left(U^1\right), \quad \vartheta_e^2 = \tan^{-1}\left(\frac{U^2}{2}\right). \quad (5.16)$$

$$(5.17)$$

Sector	Representation	$\alpha' \cdot mass^2$
aa^*	$10(3, 1)_{1/3} + 8(6, 1)_{-1/3}$	$\pm \left(-1 + \frac{1}{\pi}\tan^{-1}\left(\frac{U^1}{3}\right) - \frac{1}{\pi}\tan^{-1}\left(\frac{U^2}{6}\right)\right)$
dd^*	$4(1, 1)_{-1}$	$\pm \frac{1}{\pi} \left(-\tan^{-1}\left(\frac{2U^1}{3}\right) + \tan^{-1}\left(\frac{U^2}{2}\right)\right)$
ee^*	No scalars present	
ad	$18(3, 1)_{-2/3}$	$\pm \frac{1}{2} \left[\frac{1}{\pi}\tan^{-1}\left(\frac{U^1}{3}\right) - \frac{1}{\pi}\tan^{-1}\left(\frac{U^2}{6}\right) + \frac{1}{\pi}\tan^{-1}\left(\frac{U^2}{2}\right) - \frac{1}{\pi}\tan^{-1}\left(\frac{2U^1}{3}\right)\right]$
ad^*	$3(3, 1)_{-1/3}$	$\pm \frac{1}{2\pi} \left[-\pi + \tan^{-1}\left(\frac{U^2}{2}\right) - \tan^{-1}\left(\frac{2U^1}{3}\right) + \tan^{-1}\left(\frac{U^1}{3}\right) - \tan^{-1}\left(\frac{U^2}{6}\right)\right]$
ae^*	$2(3, 1)_{1/3}$	$\pm \frac{1}{2\pi} \left[-\pi + \tan^{-1}\left(\frac{U^1}{3}\right) + \tan^{-1}\left(\frac{U^2}{2}\right) - \tan^{-1}\left(\frac{U^2}{6}\right) - \tan^{-1}(U^1)\right]$
ae	$8(3, 1)_{-2/3}$	$\pm \frac{1}{2\pi} \left[-\pi - \tan^{-1}\left(\frac{2U^2}{3}\right) + \tan^{-1}\left(\frac{U^2}{2}\right) + \tan^{-1}\left(\frac{U^1}{3}\right) + \tan^{-1}(U^1)\right]$
de	$(1, 1)_0$	$\pm \frac{1}{2\pi} \left(-\tan^{-1}\left(\frac{2U^1}{3}\right) + \tan^{-1}(U^1)\right) + \frac{Z^2}{4\pi^2}$
de^*	$5(1, 1)_0$	$\pm \frac{1}{2\pi} \left(-\tan^{-1}(U^1) - \tan^{-1}\left(\frac{2U^1}{3}\right) + 2\tan^{-1}\left(\frac{U^2}{2}\right)\right)$

Table 24: Lightest scalar excitations for the A1-quiver models. The subscript denotes the hypercharge.

As can be seen from table (24) there is a number of scalars present in the models. These scalars may receive, as the models are non-SUSY, important higher loop corrections which are stronger for coloured scalars. As it has been emphasized before [19, 2], the precise form of the one loop corrections takes the form

$$\Delta m^2(\mu) = \sum_a \frac{4C_F^a \alpha_a(M_s)}{4\pi} M_s^2 f_a \log(M_s/\mu) \Delta M_{KK/W}^2, \quad (5.18)$$

where $t = 2 \log(M_s/\mu)$ and b_a the one-loop β -function coefficients, C_F^a the quadratic Casimir in the fundamental representation and the sum over the index a runs over the different gauge representation of the individual scalar fields. Also, $\Delta M_{KK/W}^2$ receives contributions from Kaluza-Klein, winding and string excitations lighter than the string scale¹². Thus all scalars in the models are expected to receive non-zero contributions to their mass, the latter being driven to positive values for these scalars.

The complete absence of tachyons in the models is difficult to be maintained just by fixing the complex structure parameter. E.g. the choice

$$\frac{2U^1}{3} = \frac{U^2}{2}, \quad (5.19)$$

sends to zero the mass of the dd^* scalars. Also the mass of the de-sector singlet scalars may become positive by varying the distance between the branes. In addition, all scalars receive corrections from (5.18). Thus the A1-models may receive important loop corrections which may lift their tachyonic directions. Our claim will be further justified in section 7, where the models will be shown to be equivalent to the four stack $a1$ quivers under brane recombination. A comment is in order. From the ee^* sector there are no scalars present, as can be seen from the fact that the “existing” scalars transform in the antisymmetric representation of the $U(1)$ group.

5.4 Vacua from the Five-Stack $\overline{A1}$ -type quiver

In this section we examine the derivation of a class of Standard models with exactly the SM at low energies, from the embedding of the five stack SM structure of table (2) in the quiver of $\overline{A1}$ -type.

The solutions satisfying simultaneously the intersection constraints and the cancellation of the RR twisted crosscap tadpole cancellation constraints are given in parametric form in table (25). These solutions represent the most general solution of the RR tadpoles. The twisted RR solutions of table (25) satisfy all tadpole equations in (2.16), but the first. The latter reads :

$$9n_a^1 - \frac{1}{\beta^1} + n_a^1 \tilde{\epsilon} + n_e^1 \tilde{\epsilon} + \frac{2\epsilon_h N_h}{\beta^1} = -8. \quad (5.20)$$

Note that we had added the presence of extra N_h branes. Their contribution to the RR tadpole conditions is best described by placing them in the three-factorizable cycle

$$N_h (\epsilon_h/\beta_1, 0) (2, 0) 1_{N_h} . \quad (5.21)$$

¹²Where $f_a = \frac{2+b_a \frac{\alpha_a(M_s)}{4\pi} t}{1+b_a \frac{\alpha_a(M_s)}{4\pi} t}$, and b_a the coefficients of the one-loop β -functions.

N_i	(n_i^1, m_i^1)	(n_i^2, m_i^2)	(n_i^3, m_i^3)
$N_a = 3$	$(n_a^1, \epsilon \tilde{\epsilon} \beta^1)$	$(3, \frac{1}{2} \tilde{\epsilon} \epsilon)$	1_3
$N_b = 2$	$(1/\beta_1, 0)$	$(1, \frac{1}{2} \epsilon \tilde{\epsilon})$	$\alpha^2 \mathbf{1}_2$
$N_c = 1$	$(1/\beta_1, 0)$	$(0, -\epsilon \tilde{\epsilon})$	α^2
$N_d = 1$	$(n_d^1, 2\epsilon \beta^1)$	$(\tilde{\epsilon}, -\frac{1}{2} \epsilon)$	1
$N_e = 1$	$(n_e^1, \epsilon \beta^1)$	$(\tilde{\epsilon}, -\frac{1}{2} \epsilon)$	1
N_h	$(\epsilon_h/\beta^1, 0)$	$(2, 0)$	1_{N_h}

Table 25: General tadpole solutions for the five-stack $\overline{A1}$ -type quiver of intersecting D5-branes, giving rise to exactly the standard model to low energies. The solutions depend on three integer parameters, n_a^1 , n_d^1 , n_e^1 , the NS-background β^1 and the phase parameters $\epsilon = \tilde{\epsilon} = \pm 1$, as well as the CP phase α .

The presence of an arbitrary number of N_h D5-branes, which give an extra $U(N_h)$ gauge group, don't make any contribution to the rest of the tadpoles and intersection constraints. Thus in terms of the low energy theory their presence has no effect. The $U(1)$ couplings to twisted RR fields read:

$$\begin{aligned}
& B_2^{(1)} \wedge c_1 [2 \frac{(\alpha^2 - \alpha)}{\beta^1}] F^b, \\
& D_2^{(1)} \wedge c_1 [\epsilon \tilde{\epsilon}] [3n_a^1 F^a - \frac{1}{\beta^1} F^b + \frac{1}{\beta^1} F^c - \tilde{\epsilon} n_d^1 F^d - \tilde{\epsilon} n_e^1 F^e], \\
& E_2^{(1)} \wedge c_1 [2\epsilon \tilde{\epsilon} \beta^1] [9F^a + 2F^d + F^e].
\end{aligned} \tag{5.22}$$

The combination of the $U(1)$'s which remains light at low energies is given by

$$Q^l = (Q_a - 3Q_d - 3Q_e) - 3\beta^1(n_a^1 + \tilde{\epsilon} n_d^1 + \tilde{\epsilon} n_e^1) Q_c. \tag{5.23}$$

In addition, the hypercharge condition in this case is given uniquely by

$$\beta^1(n_a^1 + \tilde{\epsilon} n_d^1 + \tilde{\epsilon} n_e^1) = 1. \tag{5.24}$$

The, other than hypercharge, anomaly free, $U(1)$ is given by

$$Q^{(5)} = (Q_d - 2Q_e + Q_c). \tag{5.25}$$

Using the condition coming from the requirement the fifth $U(1)$ to survive massless the Green-Schwarz mechanism, e.g. if it is orthogonal to the model dependent $U(1)$ coupled to the RR field $D_2^{(1)}$ give us $(1/\beta_1) - \tilde{\epsilon}n_d^1 + 2\tilde{\epsilon}n_e^1 = 0$. Wrappings consistent with this constraint and (5.20) are given by

$$n_d = 4, \quad n_e = 3, \quad \tilde{\epsilon} = -1, \quad \beta_1 = 1/2, \quad \epsilon = 1, \quad \epsilon_h = 1, \quad N_h = 20, \quad n_a^1 = 9. \quad (5.26)$$

If the scalar fields $(1, 1)_0$, which are localized in the de -sector with mass given by ¹³

$$\alpha' m_{de}^2 = \pm \frac{1}{2\pi} \left| \tan^{-1}\left(\frac{U^1}{4}\right) - \tan^{-1}\left(\frac{U^1}{6}\right) \right| + \frac{\bar{Z}^{(2)}}{4\pi^2}, \quad (5.27)$$

receive a vev then they may break the $Q^{(5)}$ symmetry. All scalars that may be present in the models may receive important loop corrections from (5.18) which may lift their tachyonic directions. Thus at low energies only the SM gauge group survives.

5.5 SM Vacua from the Five-Stack A2-type quiver

In this section we examine the derivation of a class of theories with exactly the SM at low energies. They come from the embedding of the five stack SM structure of table (2) in the quiver of A2-type.

With the choice of tadpole solutions of table (26) all tadpole solutions in (2.16), but the first, are satisfied, the latter giving

$$9n_a^1 - \frac{\tilde{\epsilon}}{\beta^1} + n_d^1 + n_e^1 + \frac{2\epsilon_h N_h}{\beta^1} = -8. \quad (5.28)$$

The $U(1)$ couplings to twisted RR fields read:

$$\begin{aligned} B_2^{(1)} &\wedge c_1 \left[-2\tilde{\epsilon} \frac{\alpha - \alpha^2}{\beta^1} \right] F^b, \\ D_2^{(1)} &\wedge c_1 [\tilde{\epsilon}\epsilon] \left[3n_a^1 F^a - \frac{\tilde{\epsilon}}{\beta^1} F^b - \frac{\tilde{\epsilon}}{\beta^1} F^c - n_d^1 F^d - n_e^1 F^e \right], \\ E_2^{(1)} &\wedge c_1 (-2\epsilon\beta^1) [9F^a + 2F^d + F^e]. \end{aligned} \quad (5.29)$$

The combination of the $U(1)$'s which remains light at low energies is given by

$$Q^l = (Q_a - 3Q_d - 3Q_e) + 3\tilde{\epsilon}\beta^1(n_a^1 + n_d^1 + n_e^1)Q_c. \quad (5.30)$$

while the hypercharge condition in this case is given uniquely by

$$\tilde{\epsilon}\beta^1(n_a^1 + n_d^1 + n_e^1) = -1. \quad (5.31)$$

¹³where $\bar{Z}^{(2)}$ is the transverse distance between the branes d, e in the second tori

N_i	(n_i^1, m_i^1)	(n_i^2, m_i^2)	(n_i^3, m_i^3)
$N_a = 3$	$(n_a^1, -\epsilon\beta^1)$	$(3, \frac{1}{2}\tilde{\epsilon}\epsilon)$	1_3
$N_b = 2$	$(1/\beta_1, 0)$	$(\tilde{\epsilon}, \frac{1}{2}\epsilon)$	$\alpha 1_2$
$N_c = 1$	$(1/\beta_1, 0)$	$(0, \epsilon)$	α^2
$N_d = 1$	$(n_d^1, -2\epsilon\beta^1)$	$(1, -\frac{1}{2}\epsilon\tilde{\epsilon})$	1
$N_e = 1$	$(n_e^1, -\epsilon\beta^1)$	$(1, -\frac{1}{2}\epsilon\tilde{\epsilon})$	1
N_h	$(\epsilon_h/\beta^1, 0)$	$(2, 0)$	1_{N_h}

Table 26: General tadpole solutions for the five-stack A2-type quiver of intersecting D5-branes, giving rise to the standard model at low energies. The solutions depend on three integer parameters, n_a^1, n_d^1, n_e^1 , the NS-background β^1 and the phase parameters $\epsilon = \tilde{\epsilon} = \pm 1$, as well as the CP phase α .

The fifth anomaly free $U(1)$ given by

$$Q^{(5)} = (Q_d - 2Q_e + Q_c) \quad (5.32)$$

survives massless the generalized Green-Schwarz mechanism if $-n_d^1 + 2n_e^1 - \tilde{\epsilon}/\beta^1 = 0$. Wrapping numbers consistent with this constraint and (5.28) are given by

$$n_e^1 = 1, n_a^1 = -3, n_d^1 = 4, \beta_1 = 1/2, \epsilon = 1, \tilde{\epsilon} = 1, \epsilon_h = 1, N_h = 3. \quad (5.33)$$

Then $U(1)$ gauge boson associated with (5.32) gets broken with the help of de -sector scalars

$$(1, 1)_0 \quad (5.34)$$

with

$$\alpha' m_{de}^2 = \pm \frac{1}{2\pi} \left(-\frac{1}{\pi} \tan^{-1}\left(\frac{U^1}{4}\right) + \tan^{-1}\left(\frac{U^1}{2}\right) \right) + \frac{\bar{Z}^2}{4\pi^2}, \quad (5.35)$$

where \bar{Z} is the distance between the branes d, e in the second tori. The latter scalars receive a vev and break the $Q^{(5)}$ symmetry leaving only the SM gauge symmetry at low energies. Any tachyonic directions that may be present in the models may receive important corrections from the couplings (5.18).

N_i	(n_i^1, m_i^1)	(n_i^2, m_i^2)	(n_i^3, m_i^3)
$N_a = 3$	$(n_a^1, \epsilon \tilde{\epsilon} \beta^1)$	$(3, \frac{1}{2} \tilde{\epsilon} \epsilon)$	1_3
$N_b = 2$	$(1/\beta_1, 0)$	$(1, \frac{1}{2} \tilde{\epsilon} \epsilon)$	$\alpha^2 \mathbf{1}_2$
$N_c = 1$	$(1/\beta_1, 0)$	$(0, \epsilon \tilde{\epsilon})$	α
$N_d = 1$	$(n_d^1, 2\epsilon \beta^1)$	$(\tilde{\epsilon}, -\frac{1}{2} \epsilon)$	1
$N_e = 1$	$(n_e^1, \epsilon \beta^1)$	$(\tilde{\epsilon}, -\frac{1}{2} \epsilon)$	1
N_h	$(\epsilon_h/\beta^1, 0)$	$(2, 0)$	1_{N_h}

Table 27: General tadpole solutions for the five-stack $\overline{A2}$ -type quiver of intersecting D5-branes, giving rise to the standard model at low energies. The solutions depend on three integer parameters, n_a^1, n_d^1, n_e^1 , the NS-background β^1 and the phase parameters $\epsilon = \tilde{\epsilon} = \pm 1$, as well as the CP phase α .

5.6 SM Vacua from the Five-Stack $\overline{A2}$ -type quiver

In this section we examine the derivation of a class of models, with exactly the SM at low energies, from the embedding of the five stack SM structure of table (2) in the quiver of $\overline{A2}$ -type. With the choice of tadpole solutions of table (27) all tadpole solutions in (2.16), but the first, are satisfied, the latter giving

$$9n_a^1 - \frac{1}{\beta^1} + \tilde{\epsilon}(n_d^1 + n_e^1) + \frac{2\epsilon_h N_h}{\beta^1} = -8. \quad (5.36)$$

The $U(1)$ couplings to twisted RR fields read

$$\begin{aligned}
& B_2^{(1)} \wedge c_1 \left[-2 \frac{\alpha - \alpha^2}{\beta^1} \right] F^b, \\
& D_2^{(1)} \wedge c_1 [\tilde{\epsilon} \epsilon] \left[3n_a^1 F^a - \frac{1}{\beta^1} F^b - \frac{1}{\beta^1} F^c - \tilde{\epsilon} n_d^1 F^d - \tilde{\epsilon} n_e^1 F^e \right], \\
& E_2^{(1)} \wedge c_1 [2\epsilon \epsilon \beta^1] [9F^a + 2F^d + F^e].
\end{aligned} \quad (5.37)$$

The combination of the $U(1)$'s which remains light at low energies is given by

$$Q^l = (Q_a - 3Q_d - 3Q_e) + 3\beta^1(n_a^1 + \tilde{\epsilon}n_d^1 + \tilde{\epsilon}n_e^1)Q_c. \quad (5.38)$$

The hypercharge condition in this case is given uniquely by

$$\beta^1(n_a^1 + \tilde{\epsilon}n_d^1 + \tilde{\epsilon}n_e^1) = -1 \quad (5.39)$$

The other anomaly free $U(1)$, beyond hypercharge, given by

$$Q^{(5)} = Q_d - 2Q_e + Q_c \quad (5.40)$$

survive massless the Green-Schwarz mechanism if $-n_d^1 + 2n_e^1 - (\tilde{\epsilon}/\beta^1) = 0$. A set of wrappings consistent with the last constraint and (5.36) are given by

$$n_a^1 = 3, \quad n_d = 4, \quad n_e = 1, \quad \tilde{\epsilon} = -1, \quad \epsilon = 1, \quad \epsilon_h = 1, \quad N_h = 1. \quad \beta^1 = 1/2. \quad (5.41)$$

The scalar fields breaking $Q^{(5)}$ get localized in the de -sector, e.g. $(1,1)_0$ with mass given by

$$\alpha' m_{de}^2 = \pm \frac{1}{2\pi} \left| \tan^{-1}\left(\frac{U^1}{4}\right) - \tan^{-1}\left(\frac{U^1}{2}\right) \right| + \frac{\bar{Z}^{(2)}}{4\pi^2}, \quad (5.42)$$

where $\bar{Z}^{(2)}$ is the transverse distance between the branes d, e in the second tori. The latter scalars receive a vev and break the $Q^{(5)}$ symmetry. Tachyonic scalar directions may be lifted by their corrections from the couplings (5.18). Thus at low energy we get the SM gauge group and chiral content.

6 Standard Models from Six-Stack Z_3 Quivers

In this section, we discuss the embedding of SM configurations of table (3) in six stacks of intersecting D5-branes at the string scale, that in general, give at low energy the SM together with some extra scalar fields. Part of these scalar fields is responsible for breaking the two anomaly free free $U(1)$'s, beyond the the $U(1)$ corresponding to the SM, surviving massless the generalized Green-Schwarz mechanism. Nevertheless, all scalars may receive important loop corrections from (5.18) which may lift all their tachyonic directions. The latter will be further justified in section 7 using brane recombination. The embedding of the six stack SM structure of table (3) in various quivers can be seen in figures (4) and (6). In the present work, we will describe explicitly only the C1, C2 quivers. Similar results hold for the other six stack quivers. in addition to various doublet scalar fields. However, in the next section we will show by using brane recombination that there is continuous flow of all the six stack quivers to their four stack quiver ‘counterparts’.

6.1 SM Vacua from the Six-Stack C1-quiver

The C1-quiver of SM embedding seen in figure (3) is solved by the RR tadpole solutions seen in Appendix III. With the latter choice the tadpole solutions in (2.16), but the

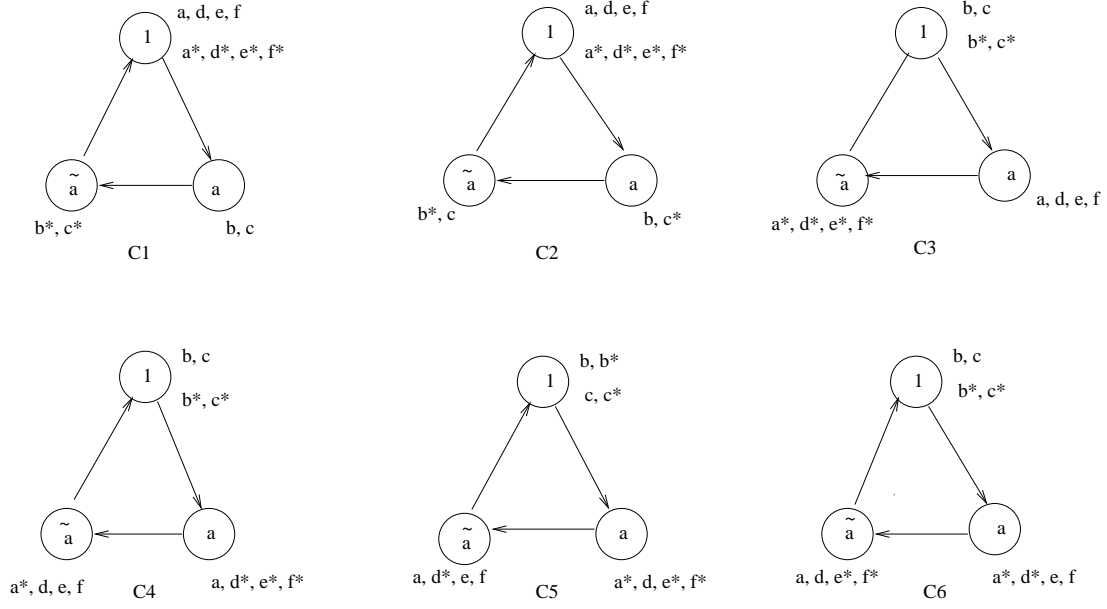


Figure 4: Assignment of SM embedding in configurations of six stacks of D5 branes depicted in Z_3 quiver diagrams; six out of a total of ten quivers. In all the cases we get the SM at low energy. Note that $\tilde{\alpha} = \alpha^{-1}$.

first, are satisfied, the latter giving

$$9n_a^1 - \frac{\tilde{\epsilon}}{\beta^1} + n_d^1 + n_e^1 + n_f^1 + \frac{2\epsilon_h N_h}{\beta^1} = -8. \quad (6.1)$$

Also the $U(1)$ couplings to twisted RR fields read:

$$\begin{aligned} B_2^{(1)} &\wedge c_1 \left[2\tilde{\epsilon} \frac{\alpha - \alpha^2}{\beta^1} \right] F^b, \\ D_2^{(1)} &\wedge c_1 [\tilde{\epsilon}\epsilon] \left[3n_a^1 F^a - \frac{\tilde{\epsilon}}{\beta^1} F^b + \frac{\tilde{\epsilon}}{\beta^1} F^c - n_d^1 F^d - n_e^1 F^e - n_f^1 F^f \right], \\ E_2^{(1)} &\wedge c_1 (-2\epsilon\beta^1) [9F^a + F^d + F^e + F^f]. \end{aligned} \quad (6.2)$$

There are three $U(1)$'s which survive massless the Green-Schwarz mechanism. One of them is automatically orthogonal to all $U(1)$'s seen in (6.2). It is

$$Q^l = (Q_a - 3Q_d - 3Q_e - 3Q_f) - 3\tilde{\epsilon}\beta^1 (n_a^1 + n_d^1 + n_e^1 + n_f^1) Q_c. \quad (6.3)$$

The latter $U(1)$ represents the hypercharge (3.6) if the hypercharge condition is satisfied

$$\tilde{\epsilon}\beta^1 (n_a^1 + n_d^1 + n_e^1 + n_f^1) = 1. \quad (6.4)$$

The other $U(1)$'s which survive massless the Green-Schwarz mechanism are given by

$$Q^{(5)} = 2Q_d - Q_e - Q_f, \quad (6.5)$$

$$Q^{(6)} = Q_e - Q_f \quad (6.6)$$

The $U(1)$'s (6.6) remain massless, and orthogonal to the $U(1)$'s (6.2) if $n_d^1 = n_e^1 = n_f^1$. The set of wrappings

$$n_a^1 = 4, n_d^1 = n_e^1 = n_f^1 = -1, \beta^1 = 1, \tilde{\epsilon} = 1, \epsilon_h = -1, N_h = 20 \quad (6.7)$$

is consistent with all the constraints present.

The scalars from the de^* sector

$$I_{de^*}(1, 1)_0 \equiv 2(1, 1)_0 \quad (6.8)$$

break the extra $U(1)$ $Q^{(5)}$. Also the scalars from the df^* sector

$$I_{df^*}(1, 1)_0 \equiv 2(1, 1)_0 \quad (6.9)$$

break the extra $U(1)$ $Q^{(6)}$. The masses of the de^* , df^* scalars may be given respectively by

$$\alpha' m_{de^*}^2 = \pm |1 - \frac{1}{\pi} \tan^{-1}(U^1) - \frac{1}{\pi} \tan^{-1}(\frac{U^2}{2})|, \quad (6.10)$$

$$m_{df^*}^2 = m_{de^*}^2 \quad (6.11)$$

Because all scalars receive important corrections to their mass from the couplings (5.18) all tachyonic directions may be lifted. Thus at low energies, only the SM survives.

6.2 SM Vacua from the Six-Stack C2-quiver

The C2-quiver embedding of the SM chiral fermions of table (3) can be seen in figure (4). With the choice of tadpole solutions seen in appendix C all tadpole solutions in (2.16), but the first, are satisfied, the latter giving

$$9n_a^1 - \frac{1}{\beta^1} + n_d^1 + n_e^1 + n_f^1 + \frac{2\epsilon_h N_h}{\beta^1} = -8. \quad (6.12)$$

The $U(1)$ couplings to twisted RR fields follows:

$$\begin{aligned} B_2^{(1)} &\wedge c_1[2\frac{\alpha - \alpha^2}{\beta^1}]F^b, \\ D_2^{(1)} &\wedge c_1[\tilde{\epsilon}\epsilon][3n_a^1 F^a - \frac{1}{\beta^1}F^b - \frac{1}{\beta^1}F^c - n_d^1 F^d - n_e^1 F^e - n_f^1 F^f], \\ E_2^{(1)} &\wedge c_1(-2\epsilon\epsilon\beta^1)[9F^a + F^d + F^e + F^f]. \end{aligned} \quad (6.13)$$

For the C2 quiver the SM hypercharge may be associated with the $U(1)$ combination

$$Q^l = (Q_a - 3Q_d - 3Q_e - 3Q_f) + 3\beta^1(n_a^1 + n_d^1 + n_e^1 + n_f^1)Q_c. \quad (6.14)$$

if the hypercharge condition is given uniquely by

$$\beta^1(n_a^1 + n_d^1 + n_e^1 + n_f^1) = -1. \quad (6.15)$$

The other $U(1)$'s which survive massless the Green-Schwarz mechanisms are given by

$$Q^{(5)} = (2Q_d - Q_e - Q_f), \quad (6.16)$$

$$Q^{(6)} = Q_e - Q_f \quad (6.17)$$

The existence of the latter $U(1)$'s give us the model dependent condition $n_d^1 = n_e^1 = n_f^1$. E.g making the choice $n_d^1 = n_e^1 = n_f^1 = 1$, $n_a^1 = -4$, $\epsilon = 1$, $\beta^1 = 1$, $\epsilon_h = -1$, $N_h = 21$, the scalars from de^* -sector $2(1, 1)_0$ break $Q^{(5)}$, while the scalars from df^* -sector $2(1, 1)_0$ break $Q^{(6)}$. Thus at low energy only the SM remains as all tachyonic directions may be lifted by the corrections (5.18).

7 Brane recombination flows of SM string vacua with different number of stacks

We have seen that when examining five and six stack vacua, some additional features appeared in comparison to the corresponding four stack ‘counterpart’ quiver vacuum¹⁴. Thus we find more scalars to be present in these models. We should emphasize however, that this is an artifact of our procedure. The appearance of the scalar spectrum in the models we studied, as opposed to the chiral multiplets that is fixed by the intersection numbers, depends on our choice of wrapping numbers entering the RR tadpole cancellation conditions. Their number for a general brane j comes from the sector which the brane transforms with a CP phase of unity.

In this section we will show that the appearance of fermion and scalars in five and six stack quiver models is in one to one correspondence with their counterpart four stack quivers. That is we show using the mechanism of brane recombination (BR), that there are directions in homology space such that the five and six stack D5 vacua are equivalent to four stack vacua and thus have only the SM at low energy.

¹⁴By ‘counterpart’ we mean the quiver obtained by ‘naively’ deleting the extra branes from the five, six, stack quivers so that they become four stack one’s.

Brane recombination in the picture of the D5-brane models we are examining may correspond exactly to the picture suggested by Sen, namely that the tachyon condensed at its minimum is exactly the final configuration of the recombined branes (which are stretched along a minimal volume cycle in its homology class). In the context of intersecting branes BR effects have been considered in [19] (and further in [24]) where it corresponds to a stringy version of the electroweak symmetry breaking mechanism. In this case it was the recombination of one of the U(1) of the ‘left’ b-brane with the U(1) ‘right’ c-brane that induced the Higgs mechanism. In our case the origin of BR effects are different. In general the BR mechanism corresponds to recombining D5-branes wrapping different intersecting cycles. We note that the D5 branes that we will recombine are not necessarily paralld across some two dimensional tori. Thus we will be able to show that by recombining always the U(1) branes that are not involved in the QCD intersection numbers (not the a, b, c, branes) there is a continuous flow between the six, five and four stack models.

In order to illuminate our points we will examine for simplicity some examples in the five and in the six stack quivers. We note that there are two general types of quivers occuring in the present work. In the first class of quivers the coloured (or baryonic)a-brane is on the same node (transforming trivially under CP) with another two d, e (resp. three, the d, e, f) U(1) branes (and/or images) in the five (resp. six) stack quiver. In the second class of quivers the left U(2) b, brane (and/or images) is on the node (transforming trivially under CP) with the right c brane (and/or images).

7.1 Five stack D5-models flowing to four stack SM D5’s

Take for example one representative of the 1st type of quivers, e.g. the five stack A1-quiver. Its intersection numbers before BR were given in eqn. (3.8). Lets us assume that two of the branes recombine, e.g. the d with e brane into a new brane j. Thus instead of the original five stack model with a, b, c, d, e branes we are left with a four stack model made of a, b, c, j branes. The new intersection numbers are computed easily by noticing that I_{ab} is now an additive quantity, thus $I_{aj} = I_{ad} + I_{ae} = 0 + 0 = 0$, and e.g. $I_{bj} = I_{bd} + I_{be} = 2 + 1 = 3$. Thus after recombination into a single brane $d + e \rightarrow j$ we are left with the following intersection numbers

$$\begin{aligned} I_{bj} &= 3, & I_{cj} &= -3, & I_{cj^*} &= 3, \\ I_{ab} &= 1, & I_{ab^*} &= 2, & I_{ac} &= -3, & I_{ac^*} &= 3 \end{aligned} \tag{7.1}$$

which we recognize to be the intersection numbers of the four stack α_1 quiver (the quiver obtained by naively deleting the e-brane from the A1-quiver!). Pictorially

$$A1 \xrightarrow{d+e=j} a1 \quad (7.2)$$

Let us now examine a quiver of the 2nd type appearing in the present work, one representative of which is the B3-quiver seen in figure (6). Again we recombine the d, e branes ¹⁵. Its intersection numbers before BR are given by

$$\begin{aligned} I_{ab} &= -1, & I_{ab^*} &= -2, & I_{ac} &= 3, & I_{ac^*} &= 3, \\ I_{bd} &= -2, & I_{be} &= -1, & I_{cd} &= 2, & I_{cd^*} &= 2, \\ I_{ce} &= 1, & I_{ce^*} &= 1 \end{aligned} \quad (7.3)$$

After BR, $d + e \rightarrow j$ and we are left with the following intersection numbers, namely

$$\begin{aligned} I_{ab} &= -1, & I_{ab^*} &= -2, & I_{ac} &= 3, & I_{ac^*} &= 3, \\ I_{bj} &= -3, & I_{cj} &= 3, & I_{ce^*} &= 3 \end{aligned} \quad (7.4)$$

which are the intersection numbers of the four stack α_4 quiver (the quiver obtained by naively deleting the e-brane from the B3-quiver). Pictorially

$$B3 \xrightarrow{d+e=j} a4 \quad (7.5)$$

Thus something novel happens here, as the the original five stack quiver A1(resp. B3) flows into the α_1 (resp. α_4) quiver. The latter quiver has only coloured scalars and they are expected to receive strong loop corrections from the couplings (5.18). Therefore the A1-quiver (resp. B3) at low energy may have only the SM at low energy. What is BR is really telling us is that there are flat directions in the moduli space of the A1-quiver (resp. B3) which can be used to break the extra U(1) symmetry carried by the e-brane. Moreover, they confirm that we are speaking about two equivalent theories.

In addition, they confirm the uniqueness of our original choice of constructing five ¹⁶ stack deformations out of the four stack vacua of [2] by deforming around its QCD intersection number structure ¹⁷. An additional example is shown in appendix for the five stack B3 quiver.

¹⁵Even though they are transforming non-trivially with a CP phase

¹⁶These results also hold for the five stack D6 SM's of [33] which under d + e brane BR, flow to the four stack SM examples of [32], while the six stack SM's of [34] flows into the SM's of [32] under d + e + f BR.

¹⁷Following the choice of universal five stack SM intersection number ansatz of table (2).

7.2 Six stack D5-models flowing to four stack D5 SM's

Using BR in the branes d, e, f, the six stack quivers can be shown to “flow” to their corresponding quiver SM that is generated by naively deleting the presence of the branes d, e, f, from the corresponding node and replacing it by the new recombined brane. To show the latter we will consider two representative examples that are based on the C1 and C3 quivers.

The intersection numbers of the C1 quiver before BR are given by

$$\begin{aligned}
I_{ab} &= 1, & I_{ab^*} &= 2, & I_{ac} &= -3, & I_{ac^*} &= 3, \\
I_{bd} &= 1, & I_{be} &= 1, & I_{bf} &= 1, & I_{cd} &= -1 \\
I_{cd^*} &= 1, & I_{ce} &= -1, & I_{ce^*} &= 1, & I_{cf} &= -1, \\
I_{cf^*} &= 1
\end{aligned} \tag{7.6}$$

After BR, $d + e + f \rightarrow l$, one can easily see that the new intersection numbers are those of (7.1). Thus we have evident the chain transition

$$C1 \xrightarrow{d+e+f=l} a1 \tag{7.7}$$

Let us now turn our attention to the C3 quiver. In this case, the intersection numbers before BR are given by

$$\begin{aligned}
I_{ab} &= -1, & I_{ab^*} &= -2, & I_{ac} &= 3, & I_{ac^*} &= 3, \\
I_{bd} &= -1, & I_{be} &= -1, & I_{bf} &= -1, & I_{cd} &= 1 \\
I_{cd^*} &= 1, & I_{ce} &= 1, & I_{ce^*} &= 1, & I_{cf} &= 1, \\
I_{cf^*} &= 1
\end{aligned} \tag{7.8}$$

while after BR, $d + e + f \rightarrow l$, they become those of the 4-stack a4-quiver, the latter naively obtained by deleting the e, f, branes from the B3-quiver diagram.

$$C3 \xrightarrow{d+e+f=l} a4 \tag{7.9}$$

7.3 Six stack D5-models flowing to five stack SM D5's

There are more chirality non-changing transitions. We note that brane recombination as we proposed to be carried out does not change the chiral content of the models but rather by changing the positions of the chiral matter in the target space reduces also the scalar content of the models present. A more appropriate name for the transitions

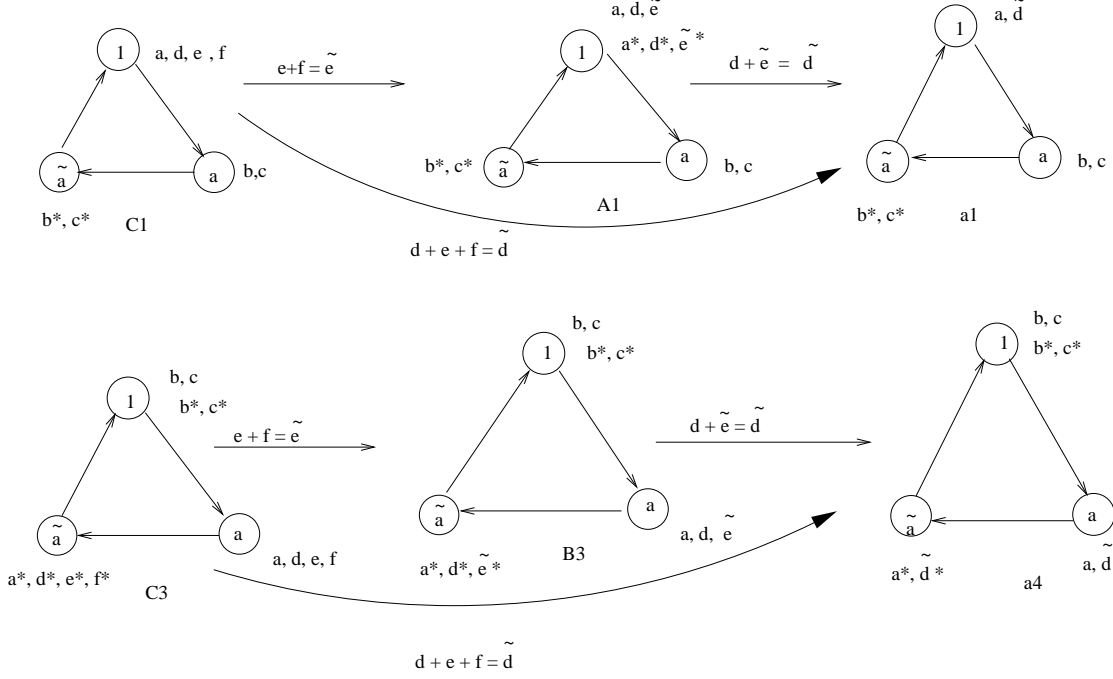


Figure 5: Recombination flow for some of the six-stack quivers. All models flow to four stack SM quivers after recombination.

taking place will be *gauge and scalar changing transitions* as they help us avoid the presence of extra scalars generically present in the five and six stack SM's.

By BR on the d, e branes under the chain $e + f \rightarrow \tilde{e}$ it may be shown that the following chirality non-changing transitions take place on the :

$$C1 \xrightarrow{e+f=\tilde{e}} B3' \quad (7.10)$$

$$C3 \xrightarrow{e+f=\tilde{e}} B3' \quad (7.11)$$

As $B3'$ quiver we denote the intersection numbers of the B3 quiver where the d, e branes are interchanged (this is a symmetry of the B3 quiver, $B3' \stackrel{d \leftrightarrow e}{\equiv} B3$). Subsequently adopting BR, $d + e \rightarrow \tilde{d}$, the $B3'$ quiver flows to the a_1 (resp. a_4) quivers. The transitions described can be seen in figure (5).

8 Epilogue

In this work, we have discussed the appearance of non-supersymmetric compactifications with D5 branes intersecting at angles that may have exactly the SM at low

energies. Our main purpose was to classify all the possible configurations that may give the SM at low energy and may be of phenomenological interest.

The models of this work, are build on a background of D5-branes, the latter being part of a four, five and six-stack structure, with intersecting D5-branes on an orientifold of $T^4 \otimes \frac{C}{\mathbb{Z}_N}$ [2]. The orbifold structure of the background is encoded in different quiver diagrams (see figures 1-7). The quiver diagrams reflect the geometric and orbifold action on the brane/orientifold-image system placed on the quiver nodes.

We completed the discussion of four stack SM's initiated in [2] by discussing the four, 'reflected', quivers Q1, Q2, Q3, Q4. We pointed out that these quivers describe equivalent theories to the quiver examples presented in [2], thus they describe vacua with exactly the SM at low energies.

We showed that reflected \mathbb{Z}_3 quivers, that are obtained from an 'image' quiver by keeping the quiver transformation of the nodes fixed, while at the same time interchanging the brane/orientifold content of the nodes with CP phases different from unity, describe equivalent theories. Also, we presented some new tadpole solutions to the four stack quivers of [2], the latter seen in figure (2). The new solutions describe, at the level of low energy effective theories equivalent SM theories to those of [2].

In addition, we discussed the Standard model embedding in five and six stack quivers, denoted as $A_i, \bar{A}_i/B_j$ ($i = 1, \dots, 2; j = 1, \dots, 7$), C_k ($k = 1, \dots, 10$) quivers respectively ¹⁸. In this case, the appearance of the SM at low energies is achieved easily but also make their appearance singlet, doublet and colour scalars. In all cases singlet scalars may be used to break the extra $U(1)$'s, while tachyonic directions that exist among scalars may be lifted by the loop corrections (5.18). Further justification to the latter was provided by using the mechanism of brane recombination (BR). BR showed us that there are gauge breaking transitions in the context of intersecting D5-branes that allow a continuous flow between the six, five and four quivers of the same kind, namely the one's that can be created by adding leptonic $U(1)$ e, f, branes, on the nodes of the four stack quiver having a baryonic (a) brane. This is quite interesting result, since gauge breaking transitions are known to exist only in the context of M-theory to occur through small instanton transitions [43].

All the models have a gauged baryon number as it happens in their orientifolded T^6 tori counterparts [33]. We note that the same property is being shared in all the constructions involving modelling with D5-branes in the same backgrounds or in the SM

¹⁸These particular SM embedding have been used before in five and six-stack orientifolded T^6 backgrounds [33, 34] respectively and produced string vacua with exactly the Standard Model at low energy.

vacua from intersecting D6-brane models on the orientifolded T^6 tori [32, 33, 34, 35]. The models based on the present backgrounds have a stability defect as they have closed string tachyons. Thus their full stability is an open question. Similar issues have been examined in the context of non-compact orbifolds [44].

Crucial for the four-, five-, six- stack constructions of D5-branes used in this work, was the configurations of tables (1), (2), (3) that exhibit the particular localization of fermions at the different intersections. The same configurations have been used before in the construction of four- five- six- stack SM's in orientifolded T^6 tori [32, 33, 34].

The most important difference of the present study with the relevant four- five or six- stack SM's found in their counterparts SM's in orientifolded T^6 tori [32, 33, 34, 35] is related to the existence of scalars in the models. In the models of [33, 34, 35] the only scalars present in the models where the one's appearing after imposing $N = 1$ SUSY in a particular sector involving the right handed neutrino. The latter supersymmetric scalars were responsible ¹⁹ for the breaking of the extra massless $U(1)$'s, beyond the one associated with the hypercharge, at low energies. On the contrary in the present intersecting brane backgrounds there is a variety of different scalars in the models, color, singlet, or doublet scalars. All scalars receive loop corrections that are stronger for the coloured scalars. Also singlet scalars are being used to break the extra $U(1)$'s, beyond hypercharge, that survive massless to low energies. The kind of scalars present in the SM-like models depends on our choice of parameters entering the RR tadpole cancellation conditions. Thus a different choice of parameters will provide us with different scalars.

In section 7, the novel use of the brane recombination (BR) mechanism showed us that there is continuous “flow” from six to five and four stack vacua depicted by quiver diagrams. In fact, we were able to show that by starting with the six stack vacua and recombining the d, e, f branes (resp. e, f) the six stack (resp. five stack) quiver intersection numbers “flow” to the four stack intersection numbers. Thus instead of solving the five and six stack quiver one could also solve the associated four stack model. As the intersection numbers I_{ab} are practically involved in the RR tadpole cancellation conditions through the relation

$$\sum_a N_a [\Pi_a] = 0 \tag{8.1}$$

¹⁹the latter scalars are necessary if the corresponding $U(1)$ gauge bosons have a zero coupling to the RR fields.

which ‘flows’ to

$$\sum_a N_a [\Pi_b] \cdot [\Pi_a] = \sum_a N_a I_{ab} = 0, \quad (8.2)$$

the latter being the cancellation of the cubic non-abelian anomalies, we have found ²⁰ that the six and five stack models are equivalent in homology space to the associated four stack models. Thus we were able to show that classes of quiver vacua with D5 branes are continuously connected ²¹. The mechanism responsible for BR flow is rather topological at our current level of understanding BR. It will be interesting if a deeper explanation may be found, perhaps in relation with a lifting of the present D5-models to their dual models that may result from an M-theory compactification. The latter perhaps could be justified in relation to the analysis of [43].

We also note that the Standard Models discussed in this work, have a natural low scale of order of the TeV [2, 14], thus avoiding the hierarchy problem, as the volume of the two dimensional manifold over which the singularity structure of C/Z_N can be embedded can be made large enough.

9 Acknowledgments

I am grateful to D. Cremades, L. Ibáñez, F. Marchesano and A. Uranga for useful discussions.

²⁰The recombination changed the intersection numbers, such the RR charge (8.1) was conserved, and (8.2) before and after recombination was preserved.

²¹It can be easily seen, using BR along the lines of section 7, that the six and five D6 brane stack deformations of [33] [34] are continuously connected to the D6-models of [32].

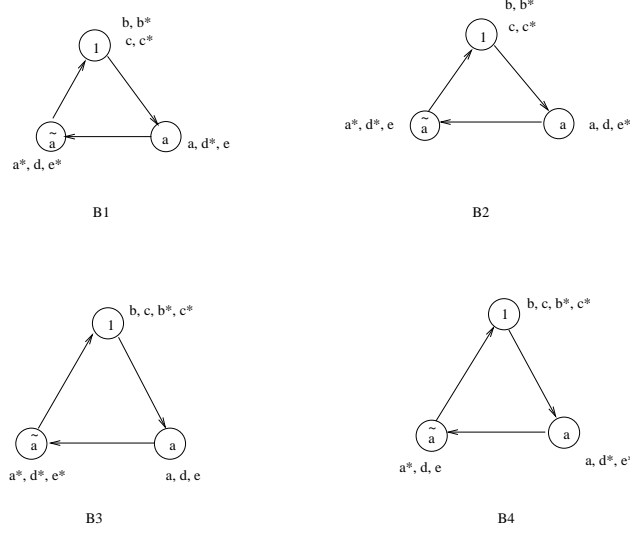


Figure 6: Configurations of D5 branes with Z_3 quiver diagrams, which give at low energy the SM.

10 Appendix A

In this appendix, we will continue the discussion of the five stack SM chiral fermion embedding of table (20), in the B1, B2, B3 quivers seen in figure 5.

10.1 SM Vacua from the five-stack B1-type quiver

This class of models is described by the embedding of the SM stack SM configurations of table (2) in the Z_3 quiver B1 seen in figure (5). The corresponding RR tadpole solutions can be seen in Appendix B.

With the choice of tadpole solutions all tadpole solutions in (2.16), but the first, are satisfied, the latter giving

$$n_b^1 = -4 + \frac{1}{\beta^1}(2 - \epsilon_h N_h) \quad (10.1)$$

The $U(1)$ couplings to twisted RR fields read

$$\begin{aligned} B_2^{(1)} \wedge c_1 \left[\frac{\alpha - \alpha^2}{\beta^1} \right] (9F^a + 2F^d + F^e), \\ D_2^{(1)} \wedge c_1 \left(-\frac{3\tilde{\epsilon}\epsilon}{2\beta^1} F^a + 2\tilde{\epsilon}\epsilon n_b^1 F^b + 2n_c^1 \epsilon F^c + \frac{\tilde{\epsilon}\epsilon}{\beta^1} F^d + \frac{\tilde{\epsilon}\epsilon}{2\beta^1} F^e \right), \\ E_2^{(1)} \wedge c_1 (-2\beta^1 \tilde{\epsilon}\epsilon) F^b. \end{aligned} \quad (10.2)$$

The combination of the $U(1)$'s which remains light at low energies is given by

$$Q^l = (Q_a - 3Q_d - 3Q_e) + \frac{3\tilde{\epsilon}}{n_c^1 \beta_1} Q_c. \quad (10.3)$$

while this $U(1)$ is identified as the hypercharge uniquely if

$$n_c^1 = -\frac{\tilde{\epsilon}}{\beta_1}. \quad (10.4)$$

We note that there is an extra anomaly free $U(1)$, beyond hypercharge, which is

$$Q^{(5)} = -\frac{3}{28}Q_a + Q_d - \frac{29}{28}Q_e - \frac{9}{28}\frac{1}{\beta_1 n_b^1}Q_b \quad (10.5)$$

The scalars from the bb^* sector break the $Q^{(5)}$ symmetry. Thus at low energy only the SM gauge group survives. Choosing $n_b^1 = 1$, $\epsilon_h = -1$, $N_h = 3$, $\epsilon\tilde{\epsilon} = 1$, $n_c^1 = 1$, we find the scalars

Sector	Representation	$\alpha' \cdot mass^2$
bb^*	$2(1,1)_{(0,2,0,0,0)}$	$\pm \frac{1}{\pi} \left(-\tan^{-1}(U^1) + \tan^{-1}(\frac{U^2}{2}) \right)$
cc^*	$2(1,1)_1$	$\pm \frac{1}{\pi} \left(\tan^{-1}(U^1) - \frac{\pi}{2} \right) + \frac{Z^2}{4\pi^2}$
bc^*	$2(2,1)_{-1/2}$	$\pm \frac{1}{2\pi} \left(-\tan^{-1}(\frac{U^1}{2}) - \tan^{-1}(U^2) \right)$
bc	$2(2,1)_{1/2}$	$\pm \frac{1}{2\pi} \left[\tan^{-1}(\frac{U^2}{2}) + \tan^{-1}(U^2) \right] + \frac{Z^1}{4\pi^2}$

Table 28: Lightest scalar excitations for the B1-quiver models. In the last three rows we have displayed the hypercharge of the scalars.

Thus (see table (28)) when $U^1 = U^2/2 = \pi/2$, the mass of the bb^* , cc^* sector scalars tends to zero. The tachyonic directions of the bc scalars may always be lifted by varying the distance along the 1st torus, while the scalars from the bc^* sector may receive loop corrections (see 5.3) which will lift their tachyonic direction. Thus at low energies only the SM remains.

10.2 SM Vacua from the five-stack B2-type quivers

This class of models is described by the embedding of the five stack SM configurations of table (2) in the Z_3 quiver B2 seen in figure (5). The RR tadpole solutions may be located in Appendix B.

The $U(1)$ couplings to twisted RR fields read:

$$\begin{aligned}
B_2^{(1)} \wedge c_1 \left[\frac{\alpha - \alpha^2}{\beta^1} \right] (9F^a + 2F^d + F^e), \\
D_2^{(1)} \wedge c_1 \left(-\frac{3\tilde{\epsilon}\epsilon}{2\beta^1} F^a + 2\tilde{\epsilon}\epsilon n_b^1 F^b + 2n_c^1 \epsilon F^c + \frac{\tilde{\epsilon}\epsilon}{\beta^1} F^d - \frac{\tilde{\epsilon}\epsilon}{2\beta^1} F^e \right) \\
E_2^{(1)} \wedge c_1 \left(-2\tilde{\epsilon}\epsilon \beta^1 F^b \right). \tag{10.6}
\end{aligned}$$

In this way all tadpole solutions in (2.16), but the first are satisfied, the latter giving

$$n_b^1 = \frac{1}{2} \left(-8 + \frac{1}{\beta^1} (5 - 2\epsilon_h N_h) \right) \tag{10.7}$$

The combination of the $U(1)$'s which doesn't have a coupling to the RR fields is

$$Q^l = (Q_a - 3Q_d - 3Q_e) + \frac{3\tilde{\epsilon}}{2n_c^1 \beta^1} Q_c \tag{10.8}$$

and it is the hypercharge if

$$n_c^1 = -\frac{\tilde{\epsilon}}{2\beta^1}. \tag{10.9}$$

From (10.7), (10.9) we conclude that $\beta^1 = 1/2$. Also there is an extra anomaly free $U(1)$ which reads

$$Q^{(5)} = \left(-\frac{3}{28} Q_a + Q_d - \frac{29}{28} Q_c - \frac{9}{28\beta^1 n_b^1} Q_b \right) \tag{10.10}$$

The latter $U(1)$ may be broken by the bb^* -sector scalars giving the SM gauge group a low energies. The remaining scalars, as in the B1 quiver, receive corrections which lift their tachyonic directions. Thus at low energy only the SM remains.

10.3 SM Vacua from the five-stack B3-type quiver

This class of models is described by the embedding of the five stack SM configurations of table (2) in the quiver B3 seen in figure (5). The RR tadpole solutions may be placed in Appendix B.

The $U(1)$ couplings to the twisted RR fields are :

$$\begin{aligned}
B_2^{(1)} \wedge c_1 \left[\frac{\alpha - \alpha^2}{\beta^1} \right] (9F^a + 2F^d + F^e), \\
D_2^{(1)} \wedge c_1 [\tilde{\epsilon}\epsilon] \left[-\frac{3}{2\beta^1} F^a + \frac{1}{2\beta^1} F^d + \frac{1}{2\beta^1} F^e + 2n_b^1 F^b - 2n_c^1 F^c \right], \\
E_2^{(1)} \wedge c_1 \left(-4 \tilde{\epsilon}\epsilon \beta^1 F^b \right). \tag{10.11}
\end{aligned}$$

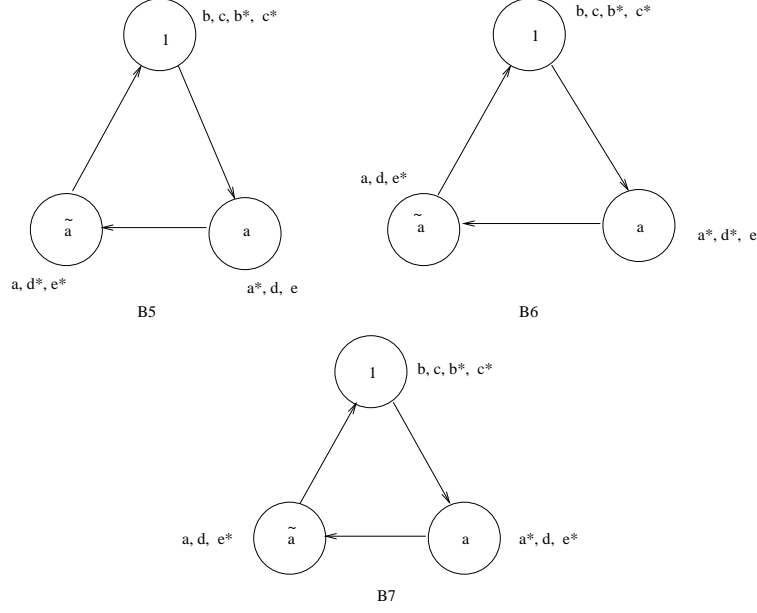


Figure 7: Configurations of five stacks of intersecting D5 branes placed in Z_3 quiver diagrams and giving rise to the SM at low energy.

Using the B3 RR tadpoles all tadpole solutions in (2.16), but the first, are satisfied, the latter giving

$$n_b^1 = -4 + \frac{1}{\beta^1}(3 - \epsilon_h N_h). \quad (10.12)$$

The $U(1)$

$$Q^l = (Q_a - 3Q_d - 3Q_e) - \frac{3}{n_c^1 \beta_1} Q_c. \quad (10.13)$$

may represent the hypercharge uniquely if

$$n_c^1 = \frac{1}{\beta^1}. \quad (10.14)$$

The other massless anomaly free $U(1)$, orthogonal to the hypercharge is

$$Q^{(5)} = \left(-\frac{3}{28}Q_a + Q_d - \frac{29}{28}Q_c - \frac{1}{14\beta^1 n_b^1}Q_b\right) \quad (10.15)$$

This $U(1)$ may be broken by the bb^* scalars, leaving the SM gauge group at low energies. The rest of the scalars will receive corrections which may lift their tachyonic directions. Actually, BR have been considered for this quiver in section (7.1) justifying our claim. Under BR the B3 quiver it has been shown in section (7.1) to be equivalent under homology flow to the $a4$ four stack quiver.

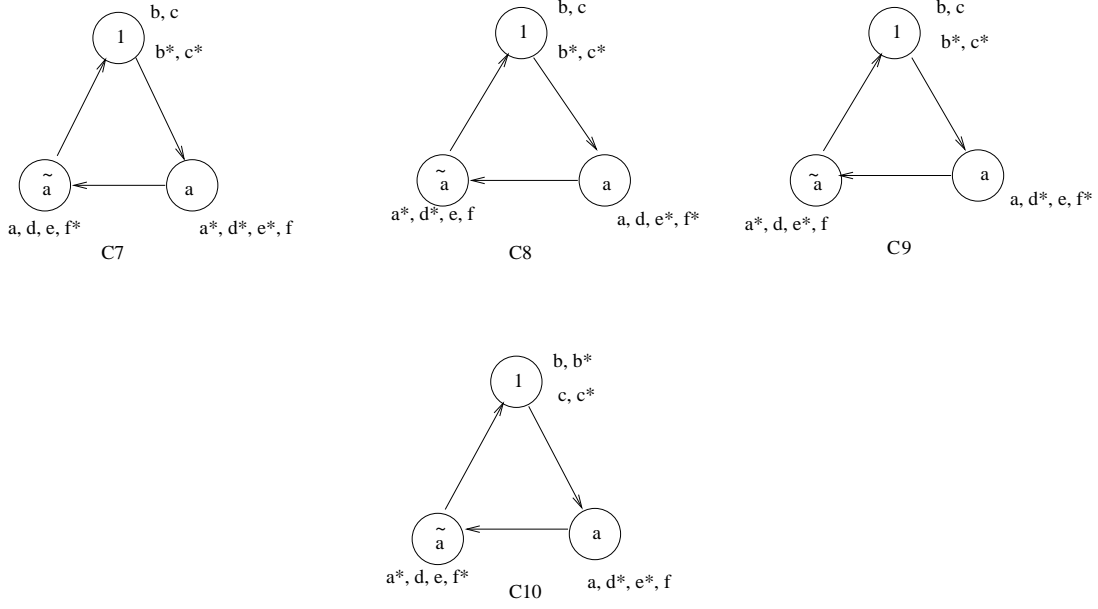


Figure 8: Assignment of SM embedding in configurations of six stacks of D5 branes depicted in Z_3 quiver diagrams; four out of a total of ten quivers, giving rise to the SM at low energy. Note that $\tilde{\alpha} = \alpha^{-1}$.

11 Appendix B

The solutions of the five stack D5 quivers depend on the integer parameters, $n_a^1, n_b^1, n_c^1, n_d^1, n_e^1$, the NS-background β^1 and the phase parameters $\epsilon = \tilde{\epsilon} = \epsilon_h = \pm 1$, also on the CP phase α .

RR tadpole solutions for B1-quiver			
N_i	(n_i^1, m_i^1)	(n_i^2, m_i^2)	(n_i^3, m_i^3)
$N_a = 3$	$(1/\beta^1, 0)$	$(3, \frac{1}{2}\tilde{\epsilon}\epsilon)$	$\alpha 1_3$
$N_b = 2$	$(n_b^1, -\tilde{\epsilon}\epsilon\beta^1)$	$(1, \frac{1}{2}\tilde{\epsilon}\epsilon)$	1_2
$N_c = 1$	$(n_c^1, \epsilon\beta^1)$	$(0, \epsilon)$	1
$N_d = 1$	$(1/\beta^1, 0)$	$(-2, \epsilon\tilde{\epsilon})$	α^2
$N_e = 1$	$(1/\beta^1, 0)$	$(1, -\frac{1}{2}\epsilon\tilde{\epsilon})$	α
N_h	$(\epsilon_h/\beta^1, 0)$	$(2, 0)$	1_{N_h}

RR tadpole solutions for B2-quiver			
N_i	(n_i^1, m_i^1)	(n_i^2, m_i^2)	(n_i^3, m_i^3)
$N_a = 3$	$(1/\beta^1, 0)$	$(3, \frac{1}{2}\tilde{\epsilon}\epsilon)$	$\alpha 1_3$
$N_b = 2$	$(n_b^1, -\tilde{\epsilon}\epsilon\beta^1)$	$(1, \frac{1}{2}\tilde{\epsilon}\epsilon)$	1_2
$N_c = 1$	$(n_c^1, \epsilon\beta^1)$	$(0, \epsilon)$	1
$N_d = 1$	$(1/\beta^1, 0)$	$(2, -\epsilon\tilde{\epsilon})$	α
$N_e = 1$	$(1/\beta^1, 0)$	$(-1, \frac{1}{2}\epsilon\tilde{\epsilon})$	α^2
N_h	$(\epsilon_h/\beta^1, 0)$	$(2, 0)$	1_{N_h}

RR tadpole solutions for B3-quiver			
N_i	(n_i^1, m_i^1)	(n_i^2, m_i^2)	(n_i^3, m_i^3)
$N_a = 3$	$(1/\beta^1, 0)$	$(3, \frac{1}{2}\tilde{\epsilon}\epsilon)$	$\alpha 1_3$
$N_b = 2$	$(n_b^1, -\tilde{\epsilon}\epsilon\beta^1)$	$(1, \frac{1}{2}\tilde{\epsilon}\epsilon)$	1_2
$N_c = 1$	$(n_c^1, -\tilde{\epsilon}\epsilon\beta^1)$	$(0, -\epsilon\tilde{\epsilon})$	1
$N_d = 1$	$(1/\beta^1, 0)$	$(2, -\epsilon\tilde{\epsilon})$	α
$N_e = 1$	$(1/\beta^1, 0)$	$(1, -\frac{1}{2}\epsilon\tilde{\epsilon})$	α
N_h	$(\epsilon_h/\beta^1, 0)$	$(2, 0)$	1_{N_h}

RR tadpole solutions for B4-quiver			
N_i	(n_i^1, m_i^1)	(n_i^2, m_i^2)	(n_i^3, m_i^3)
$N_a = 3$	$(1/\beta^1, 0)$	$(3, \frac{1}{2}\tilde{\epsilon}\epsilon)$	$\alpha 1_3$
$N_b = 2$	$(n_b^1, -\tilde{\epsilon}\epsilon\beta^1)$	$(1, \frac{1}{2}\tilde{\epsilon}\epsilon)$	1_2
$N_c = 1$	$(n_c^1, \epsilon\beta^1)$	$(0, \epsilon)$	1
$N_d = 1$	$(1/\beta^1, 0)$	$(-2, \epsilon\tilde{\epsilon})$	α^2
$N_e = 1$	$(1/\beta^1, 0)$	$(-1, \frac{1}{2}\epsilon\tilde{\epsilon})$	α^2
N_h	$(\epsilon_h/\beta^1, 0)$	$(2, 0)$	1_{N_h}

RR tadpole solutions for B5-quiver			
N_i	(n_i^1, m_i^1)	(n_i^2, m_i^2)	(n_i^3, m_i^3)
$N_a = 3$	$(1/\beta^1, 0)$	$(3, \frac{1}{2}\tilde{\epsilon}\epsilon)$	$\alpha^2 1_3$
$N_b = 2$	$(n_b^1, \tilde{\epsilon}\epsilon\beta^1)$	$(1, \frac{1}{2}\tilde{\epsilon}\epsilon)$	1_2
$N_c = 1$	$(n_c^1, \epsilon\tilde{\epsilon}\beta^1)$	$(0, -\epsilon\tilde{\epsilon})$	1
$N_d = 1$	$(1/\beta^1, 0)$	$(-2, \epsilon\tilde{\epsilon})$	α
$N_e = 1$	$(1/\beta^1, 0)$	$(-1, \frac{1}{2}\epsilon\tilde{\epsilon})$	α
N_h	$(\epsilon_h/\beta^1, 0)$	$(2, 0)$	1_{N_h}

RR tadpole solutions for B6-quiver

N_i	(n_i^1, m_i^1)	(n_i^2, m_i^2)	(n_i^3, m_i^3)
$N_a = 3$	$(1/\beta^1, 0)$	$(3, \frac{1}{2}\tilde{\epsilon}\epsilon)$	$\alpha^2 1_3$
$N_b = 2$	$(n_b^1, \tilde{\epsilon}\epsilon\beta^1)$	$(1, \frac{1}{2}\tilde{\epsilon}\epsilon)$	1_2
$N_c = 1$	$(n_c^1, \epsilon\tilde{\epsilon}\beta^1)$	$(0, -\epsilon\tilde{\epsilon})$	1
$N_d = 1$	$(1/\beta^1, 0)$	$(2, -\epsilon\tilde{\epsilon})$	α^2
$N_e = 1$	$(1/\beta^1, 0)$	$(-1, \frac{1}{2}\epsilon\tilde{\epsilon})$	α
N_h	$(\epsilon_h/\beta^1, 0)$	$(2, 0)$	1_{N_h}

RR tadpole solutions for B7-quiver

N_i	(n_i^1, m_i^1)	(n_i^2, m_i^2)	(n_i^3, m_i^3)
$N_a = 3$	$(1/\beta^1, 0)$	$(3, \frac{1}{2}\tilde{\epsilon}\epsilon)$	$\alpha^2 1_3$
$N_b = 2$	$(n_b^1, -\tilde{\epsilon}\epsilon\beta^1)$	$(-1, -\frac{1}{2}\tilde{\epsilon}\epsilon)$	1_2
$N_c = 1$	$(n_c^1, -\epsilon\tilde{\epsilon}\beta^1)$	$(0, \epsilon\tilde{\epsilon})$	1
$N_d = 1$	$(1/\beta^1, 0)$	$(-2, \epsilon\tilde{\epsilon})$	α
$N_e = 1$	$(1/\beta^1, 0)$	$(1, -\frac{1}{2}\epsilon\tilde{\epsilon})$	α^2
N_h	$(\epsilon_h/\beta^1, 0)$	$(2, 0)$	1_{N_h}

12 Appendix C

In this Appendix, we will provide the explicit RR tadpole solutions corresponding to the classification of embedding the six stack SM configurations of table (3), using intersecting D5 models, in Z_3 quivers. We list all tadpole solutions appearing in the C1,..., C10 quivers.

RR tadpole solutions for C1-quiver			
N_i	(n_i^1, m_i^1)	(n_i^2, m_i^2)	(n_i^3, m_i^3)
$N_a = 3$	$(n_a^1, -\epsilon\beta^1)$	$(3, \frac{1}{2}\tilde{\epsilon}\epsilon)$	1_3
$N_b = 2$	$(1/\beta_1, 0)$	$(\tilde{\epsilon}, \frac{1}{2}\epsilon)$	$\alpha 1_2$
$N_c = 1$	$(1/\beta_1, 0)$	$(0, -\epsilon)$	α
$N_d = 1$	$(n_d^1, -\epsilon\beta^1)$	$(1, -\frac{1}{2}\epsilon\tilde{\epsilon})$	1
$N_e = 1$	$(n_e^1, -\epsilon\beta^1)$	$(1, -\frac{1}{2}\epsilon\tilde{\epsilon})$	1
$N_f = 1$	$(n_f^1, -\epsilon\beta^1)$	$(1, -\frac{1}{2}\epsilon\tilde{\epsilon})$	1
N_h	$(\epsilon_h/\beta^1, 0)$	$(2, 0)$	1_{N_h}

RR tadpoles for 6-stack C2 quiver			
N_i	(n_i^1, m_i^1)	(n_i^2, m_i^2)	(n_i^3, m_i^3)
$N_a = 3$	$(n_a^1, -\epsilon\tilde{\epsilon}\beta^1)$	$(3, \frac{1}{2}\tilde{\epsilon}\epsilon)$	1_3
$N_b = 2$	$(1/\beta_1, 0)$	$(1, \frac{1}{2}\epsilon\tilde{\epsilon})$	$\alpha 1_2$
$N_c = 1$	$(1/\beta_1, 0)$	$(0, \epsilon\tilde{\epsilon})$	α^2
$N_d = 1$	$(n_d^1, -\epsilon\tilde{\epsilon}\beta^1)$	$(1, -\frac{1}{2}\epsilon\tilde{\epsilon})$	1
$N_e = 1$	$(n_e^1, -\epsilon\tilde{\epsilon}\beta^1)$	$(1, -\frac{1}{2}\epsilon\tilde{\epsilon})$	1
$N_f = 1$	$(n_f^1, -\epsilon\tilde{\epsilon}\beta^1)$	$(1, -\frac{1}{2}\epsilon\tilde{\epsilon})$	1
N_h	$(\epsilon_h/\beta^1, 0)$	$(2, 0)$	1_{N_h}

RR tadpoles for 6-stack C3 quiver			
N_i	(n_i^1, m_i^1)	(n_i^2, m_i^2)	(n_i^3, m_i^3)
$N_a = 3$	$(1/\beta^1, 0)$	$(3, \frac{1}{2}\tilde{\epsilon}\epsilon)$	$\alpha 1_3$
$N_b = 2$	$(n_b^1, -\tilde{\epsilon}\epsilon\beta^1)$	$(1, \frac{1}{2}\epsilon\tilde{\epsilon})$	1_2
$N_c = 1$	$(n_c^1, -\tilde{\epsilon}\epsilon\beta^1)$	$(0, -\epsilon\tilde{\epsilon})$	1
$N_d = 1$	$(1/\beta^1, 0)$	$(1, -\frac{1}{2}\epsilon\tilde{\epsilon})$	α
$N_e = 1$	$(1/\beta^1, 0)$	$(1, -\frac{1}{2}\epsilon\tilde{\epsilon})$	α
$N_f = 1$	$(1/\beta^1, 0)$	$(1, -\frac{1}{2}\epsilon\tilde{\epsilon})$	α
N_h	$(\epsilon_h/\beta^1, 0)$	$(2, 0)$	1_{N_h}

RR tadpoles for 6-stack C4 quiver

N_i	(n_i^1, m_i^1)	(n_i^2, m_i^2)	(n_i^3, m_i^3)
$N_a = 3$	$(1/\beta^1, 0)$	$(3, \frac{1}{2}\tilde{\epsilon}\epsilon)$	$\alpha 1_3$
$N_b = 2$	$(n_b^1, -\tilde{\epsilon}\epsilon\beta^1)$	$(1, \frac{1}{2}\epsilon\tilde{\epsilon})$	1_2
$N_c = 1$	$(n_c^1, -\tilde{\epsilon}\epsilon\beta^1)$	$(0, -\epsilon\tilde{\epsilon})$	1
$N_d = 1$	$(1/\beta^1, 0)$	$(-1, \frac{1}{2}\epsilon\tilde{\epsilon})$	α^2
$N_e = 1$	$(1/\beta^1, 0)$	$(-1, \frac{1}{2}\epsilon\tilde{\epsilon})$	α^2
$N_f = 1$	$(1/\beta^1, 0)$	$(-1, \frac{1}{2}\epsilon\tilde{\epsilon})$	α^2
N_h	$(\epsilon_h/\beta^1, 0)$	$(2, 0)$	1_{N_h}

RR tadpoles for 6-stack C5 quiver

N_i	(n_i^1, m_i^1)	(n_i^2, m_i^2)	(n_i^3, m_i^3)
$N_a = 3$	$(1/\beta^1, 0)$	$(3, \frac{1}{2}\tilde{\epsilon}\epsilon)$	$\alpha^2 1_3$
$N_b = 2$	$(n_b^1, -\tilde{\epsilon}\epsilon\beta^1)$	$(-1, -\frac{1}{2}\epsilon\tilde{\epsilon})$	1_2
$N_c = 1$	$(n_c^1, -\tilde{\epsilon}\epsilon\beta^1)$	$(0, \epsilon\tilde{\epsilon})$	1
$N_d = 1$	$(1/\beta^1, 0)$	$(-1, \frac{1}{2}\epsilon\tilde{\epsilon})$	α
$N_e = 1$	$(1/\beta^1, 0)$	$(1, -\frac{1}{2}\epsilon\tilde{\epsilon})$	α^2
$N_f = 1$	$(1/\beta^1, 0)$	$(1, -\frac{1}{2}\epsilon\tilde{\epsilon})$	α^2
N_h	$(\epsilon_h/\beta^1, 0)$	$(2, 0)$	1_{N_h}

RR tadpoles for 6-stack C6 quiver

N_i	(n_i^1, m_i^1)	(n_i^2, m_i^2)	(n_i^3, m_i^3)
$N_a = 3$	$(1/\beta^1, 0)$	$(3, \frac{1}{2}\tilde{\epsilon}\epsilon)$	$\alpha^2 1_3$
$N_b = 2$	$(n_b^1, -\tilde{\epsilon}\epsilon\beta^1)$	$(-1, -\frac{1}{2}\epsilon\tilde{\epsilon})$	1_2
$N_c = 1$	$(n_c^1, -\tilde{\epsilon}\epsilon\beta^1)$	$(0, \epsilon\tilde{\epsilon})$	1
$N_d = 1$	$(1/\beta^1, 0)$	$(1, -\frac{1}{2}\epsilon\tilde{\epsilon})$	α^2
$N_e = 1$	$(1/\beta^1, 0)$	$(-1, \frac{1}{2}\epsilon\tilde{\epsilon})$	α
$N_f = 1$	$(1/\beta^1, 0)$	$(-1, \frac{1}{2}\epsilon\tilde{\epsilon})$	α
N_h	$(\epsilon_h/\beta^1, 0)$	$(2, 0)$	1_{N_h}

RR tadpoles for 6-stack C7 quiver

N_i	(n_i^1, m_i^1)	(n_i^2, m_i^2)	(n_i^3, m_i^3)
$N_a = 3$	$(1/\beta^1, 0)$	$(3, \frac{1}{2}\tilde{\epsilon}\epsilon)$	$\alpha^2 1_3$
$N_b = 2$	$(n_b^1, -\tilde{\epsilon}\epsilon\beta^1)$	$(-1, -\frac{1}{2}\epsilon\tilde{\epsilon})$	1_2
$N_c = 1$	$(n_c^1, -\tilde{\epsilon}\epsilon\beta^1)$	$(0, \epsilon\tilde{\epsilon})$	1
$N_d = 1$	$(1/\beta^1, 0)$	$(1, -\frac{1}{2}\epsilon\tilde{\epsilon})$	α^2
$N_e = 1$	$(1/\beta^1, 0)$	$(1, -\frac{1}{2}\epsilon\tilde{\epsilon})$	α^2
$N_f = 1$	$(1/\beta^1, 0)$	$(-1, \frac{1}{2}\epsilon\tilde{\epsilon})$	α
N_h	$(\epsilon_h/\beta^1, 0)$	$(2, 0)$	1_{N_h}

RR tadpoles for 6-stack C8 quiver

N_i	(n_i^1, m_i^1)	(n_i^2, m_i^2)	(n_i^3, m_i^3)
$N_a = 3$	$(1/\beta^1, 0)$	$(3, \frac{1}{2}\tilde{\epsilon}\epsilon)$	$\alpha 1_3$
$N_b = 2$	$(n_b^1, -\tilde{\epsilon}\epsilon\beta^1)$	$(1, \frac{1}{2}\epsilon\tilde{\epsilon})$	1_2
$N_c = 1$	$(n_c^1, -\tilde{\epsilon}\epsilon\beta^1)$	$(0, -\epsilon\tilde{\epsilon})$	1
$N_d = 1$	$(1/\beta^1, 0)$	$(1, -\frac{1}{2}\epsilon\tilde{\epsilon})$	α
$N_e = 1$	$(1/\beta^1, 0)$	$(-1, \frac{1}{2}\epsilon\tilde{\epsilon})$	α^2
$N_f = 1$	$(1/\beta^1, 0)$	$(-1, \frac{1}{2}\epsilon\tilde{\epsilon})$	α^2
N_h	$(\epsilon_h/\beta^1, 0)$	$(2, 0)$	1_{N_h}

RR tadpoles for 6-stack C9 quiver

N_i	(n_i^1, m_i^1)	(n_i^2, m_i^2)	(n_i^3, m_i^3)
$N_a = 3$	$(1/\beta^1, 0)$	$(3, \frac{1}{2}\tilde{\epsilon}\epsilon)$	$\alpha 1_3$
$N_b = 2$	$(n_b^1, -\tilde{\epsilon}\epsilon\beta^1)$	$(1, \frac{1}{2}\epsilon\tilde{\epsilon})$	1_2
$N_c = 1$	$(n_c^1, -\tilde{\epsilon}\epsilon\beta^1)$	$(0, -\epsilon\tilde{\epsilon})$	1
$N_d = 1$	$(1/\beta^1, 0)$	$(-1, \frac{1}{2}\epsilon\tilde{\epsilon})$	α^2
$N_e = 1$	$(1/\beta^1, 0)$	$(1, -\frac{1}{2}\epsilon\tilde{\epsilon})$	α
$N_f = 1$	$(1/\beta^1, 0)$	$(-1, \frac{1}{2}\epsilon\tilde{\epsilon})$	α^2
N_h	$(\epsilon_h/\beta^1, 0)$	$(2, 0)$	1_{N_h}

RR tadpoles for 6-stack C10 quiver			
N_i	(n_i^1, m_i^1)	(n_i^2, m_i^2)	(n_i^3, m_i^3)
$N_a = 3$	$(1/\beta^1, 0)$	$(3, \frac{1}{2}\tilde{\epsilon}\epsilon)$	$\alpha 1_3$
$N_b = 2$	$(n_b^1, -\tilde{\epsilon}\epsilon\beta^1)$	$(1, \frac{1}{2}\epsilon\tilde{\epsilon})$	1_2
$N_c = 1$	$(n_c^1, -\tilde{\epsilon}\epsilon\beta^1)$	$(0, -\epsilon\tilde{\epsilon})$	1
$N_d = 1$	$(1/\beta^1, 0)$	$(-1, \frac{1}{2}\epsilon\tilde{\epsilon})$	α^2
$N_e = 1$	$(1/\beta^1, 0)$	$(-1, \frac{1}{2}\epsilon\tilde{\epsilon})$	α^2
$N_f = 1$	$(1/\beta^1, 0)$	$(1, -\frac{1}{2}\epsilon\tilde{\epsilon})$	α
N_h	$(\epsilon_h/\beta^1, 0)$	$(2, 0)$	1_{N_h}

References

- [1] For reviews on string phenomenology see (and references there in):
L. E. Ibáñez, hep-ph/9911499;
F. Quevedo, hep-ph/9707434; hep-th/9603074;
I. Antoniadis, hep-th/0102202, E. Dudas, hep-ph/0006190;
K. Dienes, hep-ph/0004129; hep-th/9602045
- [2] D. Cremades, L. E. Ibáñez, F. Marchesano, “Standard Model at Intersecting D5-branes: Lowering the String Scale”, hep-th/0205074
- [3] R. Blumenhagen, L. Görlich, B. Körs and D. Lüst, “Noncommutative compactifications of type I strings on tori with magnetic background flux”, JHEP **0010** (2000) 006, hep-th/0007024; “Magnetic Flux in Toroidal Type I Compactification”, Fortsch. Phys. 49 (2001) 591, hep-th/0010198
- [4] R. Blumenhagen, B. Körs and D. Lüst, “Type I Strings with F and B-flux”, JHEP 0102 (2001) 030, hep-th/0012156.
- [5] L. Dixon, V. Kaplunovsky and J. Louis, Nucl Phys. B355 (1991) 649;
C. Kokorelis, “String Loop Threshold Corrections for N=1 Generalized Coxeter Orbifolds”, Nucl.Phys. B579 (2000) 267-274, hep-th/0001217 ;
D. Bailin, A. Love, W.A. Sabra, S. Thomas, “String Loop threshold corrections for Z_N Coxeter orbifolds”, Mod. Phys. Lett. A9 (1994) 67-80, hep-th/9310008;
C. Kokorelis, “Gauge and Gravitational Couplings from Modular Orbits in Orbifold Compactifications”, Phys. Lett. B477 (2000) 313, hep-th/0001062
G. L. Cardoso, D. Lüst, T. Mohaupt, “ Threshold Corrections and Symmetry Enhancement in String Compactifications”, Nucl.Phys. B450 (1995) 115-173, hep-th/9412209
- [6] G. Aldazabal, L. E. Ibanez, F. Quevedo, A. M. Uranga, “D-Branes at Singularities : A Bottom-Up Approach to the String Embedding of the Standard Model”, JHEP 0008 (2000) 002, hep-th/0005067// G. Aldazabal, L.E. Ibanez, F. Quevedo, “A D-Brane Alternative to the MSSM”, JHEP 0002 (2000) 015, hep-ph/0001083
G. Aldazabal, L.E. Ibanez, F. Quevedo and A. M. Uranga, “D-branes at singularities: A bottom-up approach to the string embedding of the Standard Model”, JHEP 0008, 002 (2002), hep-th/0005067

- [7] M. Cvetič, A. M. Uranga and J. Wang, “Discrete Wilson lines in N=1 D=4 type IIB orientifolds”, Nucl. Phys. B 595, 63 (2001), hep-th/0010091
- [8] D. Berenstein, V. Jejjala and R. G. Leigh, “The Standard Model on a D-brane”, Phys. Rev. Lett. 88, 071602 (2002), hep-ph/0105042
- [9] T. W. Kephart and H. Pas, ”Three family N=1 SUSY models from Z_n orbifolded AdS/CFT”, Phys. Lett. B522, 315 (2001), hep-ph/0109111
- [10] H. Kataoka, M. Shimojo, “ $SU(3) \times SU(2) \times U(1)$ Chiral models from Intersecting D4-/D5-branes”, hep-th/0112247;
- [11] D. Bailin, G. V. Kraniotis, A. Love, “Supersymmetric Standard Models on D-Branes”, Phys. Lett. B502 (2001) 209 hep-th/0011289
- [12] H. X. Yang, ”Standard-like models from D=4 IIB orbifolds”, hep-ph/0109111
- [13] L. F. Alday and G. Aldazabal, “In quest of ”just” the Standard Model on D-branes at a singularity”, JHEP 0205 (2002) 022 hep-th/0203129
- [14] I. Antoniadis, N. Arkadi-Hamed, S. Dimopoulos, G. Dvali, Phys. Lett. B436 (1998) 257, hep-ph/9804398; I. Antoniadis, C. Bachas, Phys. Lett. B450 (1999) 83, hep-th/9812093
- [15] M. Berkooz, M. R. Douglas, R.G. Leigh, “Branes Intersecting at Angles”, Nucl. Phys. B480 (1996) 265, hep-th/9606139
- [16] M. Bianchi, G. Pradisi and A. Sagnotti, “Toroidal compactification and symmetry breaking in open string theories,” Nucl. Phys. B **376**, 365 (1992); Z. Kakushadze, G. Shiu and S.-H. H. Tye, “Type IIB orientifolds with NS-NS antisymmetric tensor backgrounds,” Phys. Rev. D **58**, 086001 (1998). hep-th/9803141; C. Angelantonj, Nucl. Phys. B566 (2000) 126, “Comments on Open-String Orbifolds with a Non-Vanishing B_{ab} ”, hep-th/9908064
- [17] R. Blumenhagen, L. Görlisch, and B. Körs, “Asymmetric Orbifolds, non-commutative geometry and type I string vacua”, Nucl. Phys. B582 (2000) 44, hep-th/0003024
C. Angelantonj and A. Sagnotti, “Type I vacua and brane transmutation”, hep-th/00010279;
C. Angelantonj, I. Antoniadis, E. Dudas and A. Sagnotti, “Type I strings on

- magnetized orbifolds and brane transmutation”, Phys. Lett. B489 (2000) 223, hep-th/0007090
- [18] R. Blumenhagen, L. Görlich, B. Kors, “Supersymmetric Orientifolds in 6D with D-Branes at Angles”, Nucl.Phys. B569 (2000) 209, hep-th/9908130; R. Blumenhagen, L. Goerlich, B. Körs, “Supersymmetric 4D Orientifolds of Type IIA with D6-branes at Angles”, JHEP 0001 (2000) 040, hep-th/9912204
- [19] G. Aldazabal, S. Franco, L. E. Ibáñez, R. Rabadán and A. M. Uranga, “D=4 chiral string compactifications from intersecting branes”, J. Math. Phys. 42 (2001) 3103-3126, hep-th/0011073; G. Aldazabal, S. Franco, L. E. Ibáñez, R. Rabadán and A. M. Uranga, “Intersecting brane worlds”, JHEP **0102** (2001) 047, hep-ph/0011132.
- [20] S. Forste, G. Honecker, R. Schreyer, “Supersymmetric $Z_N \times Z_M$ Orientifolds in 4D with D-Branes at Angles”, Nucl.Phys. B593 (2001) 127-154, hep-th/0008250; I. V. Vancea, “Note on Four Dp-Branes at Angles”, JHEP 0104:020,2001, hep-th/0011251;
- [21] D. Bailin, G. V. Kraniotis and A. Love, “Standard-like models from intersecting D4-branes”, Phys. Lett. B530 (2002) 202, hep-th/0108131
- [22] G. Honecker, “Intersecting brane world models from D8-branes on $(T^2 \times T^4/Z_3)/\Omega\mathcal{R}_1$ type IIA orientifolds”, JHEP 0201 (2002) 025, hep-th/0201037
- [23] R. Blumenhagen, B. Körs, D. Lüst and T. Ott, “The Standard Model from Stable Intersecting Brane World Orbifolds”, Nucl. Phys. B616 (2001) 3, hep-th/0107138
- [24] D. Cremades, L. E. Ibáñez, F. 4, “SUSY Quivers, Intersecting Branes and the Modest Hierarchy Problem”, hep-th/0201205; D. Cremades, L.E. Ibanez, F. Marchesano, “Intersecting Brane Models of Particle Physics and the Higgs Mechanism”, hep-th/0203160; D. Cremades, L. E. Ibáñez, F. Marchesano, “Standard Model at Intersecting D5-branes: Lowering the string scale”, hep-th/0205074
- [25] A. M. Uranga, “D-brane, fluxes and chirality”, JHEP 0204 (2002) 016, hep-th/0201221
- [26] G. Aldazabal, L. E. Ibáñez, A.M. Uranga, “Gauging Away the Strong CP Problem”, hep-ph/0205250

- [27] L. Everett, G. Kane, S. King, S. Rigolin and L. T. Wang, “Supersymmetric Pati-Salam models from intersecting branes”, Phys. Lett. B531 (2002) 263, hep-ph/0202100
- [28] J. Ellis, P. Kanti and D.V. Nanopoulos, “ Intersecting Branes Flipped SU(5)”, Nucl.Phys. B647 (2002) 235, hep-th/0206087
- [29] R. Blumenhagen, V. Braun, B. Körs, D. Lüst, “Orientifolds of K3 and Calabi-Yau Manifolds with Intersecting D-branes”, hep-th/0206038
- [30] A. M. Uranga, “Local models for intersecting brane worlds”, JHEP 0212 (2002) 058, hep-th/0208014
- [31] M. Cvetič, G. Shiu A M. Uranga, “Chiral four dimensional $N = 1$ supersymmetric IIA orientifolds from intersecting D6 branes”, Nucl. Phys. B615 (2001) 3, hep-th/0107166; “Three family supersymmetric standard models from intersecting brane worlds”, Phys. Rev. Lett. 87 (2001) 201801, hep-th/0107143; M. Cvetič, P. Laugacker, G. Shiu, “Phenomenology of a Three family Standard-like String Model ”, hep-ph/0205252
- [32] L. E. Ibáñez, F. Marchesano and R. Rabadán, “Getting just the standard model at intersecting branes” JHEP, 0111 (2001) 002, hep-th/0105155;
- [33] C. Kokorelis, “New Standard Model Vacua from Intersecting Branes”, JHEP 0209 (2002) 029, hep-th/0205147
- [34] C. Kokorelis, “Exact Standard Model Compactifications from Intersecting Branes”, JHEP 0208 (2002) 036, hep-th/0206108
- [35] C. Kokorelis, “GUT Model Hierarchies from Intersecting Branes”, JHEP 0208 (2002) 018, hep-th/0203187
- [36] J. Pati and A. Salam, “Lepton number as the forth colour” , Phys. Rev. D10 (1974) 275
- [37] L. E. Ibáñez, R. Rabadán and A. M. Uranga, “Anomalous U(1)’s in Type I and Type IIB D=4, N=1 string vacua”, Nucl.Phys. B542 (1999) 112-138
- [38] A. Sagnotti, “A Note on the Green - Schwarz Mechanism in Open - String Theories”, Phys. Lett. B294 (1992) 196, hep-th/9210127

- [39] M. R. Douglas, G. Moore, “D-branes, Quivers, and ALE Instantons”, hep-th/9603167
- [40] C. V. Johnson, R. C. Myers, “Aspects of Type IIB Theory on ALE Spaces”, Phys.Rev. D55 (1997) 6382, hep-th/9610140
- [41] M. R. Douglas, B. R. Greene, D. R. Morrison, “Orbifold Resolution by D-Branes”, Nucl. Phys. B506 (1997) 84, hep-th/9704151
- [42] E. J. Gimon and C. V. Johnson, “ K_3 orientifolds”, Nucl. Phys. B477, 715 (1996), hep-th/9604129
- [43] B. A. Ovrut, T. Pantev, J. Park, JHEP 0005 (2000) 026, hep-th/0001133
- [44] A. Adams, J. Polchinski, E. Silverstein, “Don’t Panic! Closed String Tachyons in ALE Spacetimes”, JHEP 0110 (2001) 029, hep-th/0108075